SOVIET PHYSICS USPEKHI VOLUME 9, NUMBER 6 MAY-JUNE 1967

621.385.26

New Instruments and Measurement Methods

THE AVALANCHE-TRANSIT DIODE AND ITS USE IN MICROWAVES

A. S. TAGER

Usp. Fiz. Nauk 90, 631—666 (December 1966)

1. INTRODUCTION

A characteristic feature of the development of modern radio is the rapid introduction of semiconductor devices for microwave frequencies. Progress in this direction was attained as a result of appreciable improvement in the technology of high-frequency transistors and the development of tunnel diodes and diodes with variable capacitance (varactors). Although these devices have appeared but recently, they are already extensively used in the microwave band for high-sensitivity receivers and multiplying networks. Until recently, however, there was no effective centimeter-wavelength sėlf-oscillators capable of serving as the solid state equivalent the reflex klystron, one of the basic vacuum devices for microwaves.

This gap was filled to a considerable degree by a new semiconductor microwave device, the avalanche-transit diode (ATD), on which an entire group of microwave devices (generators, amplifiers, and frequency converters) is based.

The avalanche-transit diode was first produced in the USSR in 1959 on the basis of an effect observed by the author, namely that coherent oscillations are generated in the case of avalanche breakdown of microwave germanium diffusion diodes [1-4].

The diode was placed in a high-frequency cavity and connected to a dc circuit, as shown in Fig. 1. Microwaves were generated at negative voltages, exceeding the breakdown voltage (20—30 V) by 0.5—1.5 V, whenever direct current ranging from 0.5 10—15 mA flowed through the diode. The continuous oscillation power ranged from several times ten microwatts to several milliwatts, depending on the diode. The oscillation spectrum, depending on the current flowing through the diode and depending on the cavity tuning, ranged from near-noise to almost monochromatic. The wavelength of the oscillations ranged from 0.8 to 10 cm and depended on the dimensions of the cavity and on the values of the reactive parameters of the diodes. By tuning the cavity it was possible to vary smoothly the frequency and power of the oscillations. In the underexcited mode, near the generation threshold, regenerative amplification of the microwave oscillations was observed, with a gain 15—20 dB. The diodes with which generation and amplification of microwaves were obtained did not produce as a rule a noticeable parasitic generation at lower frequencies, although no special measures were taken to suppress it.

It became clear subsequently that microwave generation in the electric breakdown mode can be observed also in diodes of other types - silicon, alloyed germanium, etc. Recently this phenomenon was observed by American researchers in switching and parametric diodes made of silicon and gallium arsenide [5,6].

Even the first experiments have shown that the main feature of the generating diodes is the form of the inverse branch of the current-voltage characteristic, namely, a sharply pronounced breakdown voltage V_{br} and a linear increase of the current at negative voltages exceeding V_{br} (in absolute magnitude) (Fig. 2). The slope of the current-voltage characteristic in the working region was positive everywhere, with a differential resistance R_d = 50—300 ohm. As a rule, no sections with negative slope, corresponding to negative "static" diode resistance, were observed in the working mode.

For a phenomenological treatment of this effect we can ascribe to the diode a dynamic negative resistance, assuming that the active component of the total impedance of the diode is negative in a more or less narrow range of frequencies where the generation is observed, and at the remaining frequencies this resistance is positive. Let us examine qualitatively the mechanism whereby dynamic negative resistance is produced in diodes.

2. DIODES WITH DYNAMIC NEGATIVE RESISTANCE. OPERATING PRINCIPLE OF THE AVALANCHE-TRANSIT DIODE

Diodes with dynamic negative resistance have been known in vacuum electronics for more than 30

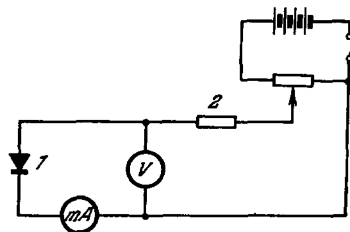

FIG. 1. Diagram showing the connection of an ATD in a dc circuit. 1 – Diode, 2 – ballast resistor.

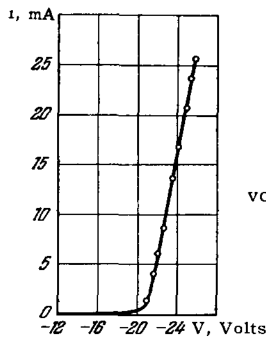

FIG. 2. Inverse branch of the current-voltage characteristic of the ATD.

years[7-9]. F. Llewellyn has shown experimentally that a microwave generator can be constructed on the basis of such a diode[10,11]. Such a generator consists of a diode gap bounded by two electrodes (cathode and anode) to which a constant potential difference V_0 and an alternating potential difference $\tilde{V}$ are applied, and an external tank circuit. An unmodulated electron beam from a thermionic cathode enters the diode gap. Under the influence of the alternating field, the electron velocity changes and the initially homogeneous electron beam becomes bunched. The average (over the cycle) of the energy of interaction between the electrons and the alternating field turns out to be different from zero and to depend on the transit angle of the electrons in the diode. In certain transit-angle intervals, $2\pi n < \xi < (2n + 1)\pi$ $(n = 1, 2, \ldots)$, this energy is negative, and in the corresponding frequency intervals it is possible to assign to the diode a negative resistance (or a negative conductance)*. However, owing to the low efficiency of this method of bunching, the absolute magnitude of the active resistance of the diode turns out to be much smaller than its reactive (capacitive) susceptance, so that in order to produce a microwave self oscillator it is necessary to connect to the diode an external high-Q tank circuit, and to draw large current densities from the cathode. Consequently the realization of such generators encountered appreciable difficulties and, in spite of the large number of theoretical papers, these generators did not find practical application.

Yet there exists a fundamentally simple method of greatly increasing the efficiency of diode generators. It consists of replacing the velocity modulation of the electron by current modulation at the input to the diode gap. Let us assume that we use in lieu of the thermionic cathode some type of field-emission cathode with sufficiently sharp dependence of the emission current on the electric field intensity. In this case the current emitted from the cathode will be density-modulated at the frequency of the applied voltage. The active resistance of such a diode can take on negative values even in the absence of additional bunching of the electrons in the diode gap. This can be clearly seen from the space-time diagram showing the motion of the electrons in a "field emission" diode* shown in Fig. 3a. The electron bunches extracted from the cathode at the instant when the high-frequency field has a maximum, first move in an accelerating field and then in a decelerating field, and if the transit angle between the cathode and the anode exceeds π, the active resistance of the diode is negative and reaches a maximum value at $\xi \simeq 3\pi/2$ (Fig. 4a).

The additional bunching of the electrons by velocity modulation in the diode gap plays in this case a secondary role. Both the excitation conditions and the efficiency of such a generator can be much better than in diode generators with velocity modulation of the electrons.

Figure 3a pertains to the case when the emission current follows instantaneously the electric field intensity. Let us assume now that for some reason the emission current lags the electric field intensity in time. If the emission delay time γT is related in definite fashion with the oscillation period T, then the efficiency of the diode generator can be even higher. Let, for example, $\gamma = 1/4 + n$ $(n = 0, 1, 2, \ldots)$. In this case, as seen from Fig. 3b, the electrons emitted from the cathode fall immediately into the decelerating high-frequency field. The dependence of the active resistance of such a diode on the electron transit angle, without allowance for the electron space charge, is shown schematically in Fig. 4b. The active resistance of the diode is negative at all transit angles, with exception of the points $\xi = 2\pi n$, and its absolute value has maximum at $\xi \simeq (2n + 1)\pi$ $(n = 0, 1, 2, \ldots)$. In the ideal case, the efficiency of such a generator can reach very high values.

In the foregoing reasoning we started from a purely kinematic model, neglecting the effect of the electron space charge in the diode gap. Yet the electron space charge, by reducing the electric field intensity at the cathode, produces in a field-emission diode a unique mechanism of internal negative feedback.

The lag of the emission current relative to the field is equivalent to introduction of delay in the negative feedback. Having definite dispersion properties, such feedback facilitates the excitation of self-oscillations in the system at certain frequencies, by relaxing the requirements with respect to the Q of the external tank circuit, and at other frequencies, to the contrary, it makes these conditions worse, even

*When speaking of resistance, we refer throughout to a series equivalent circuit of the diode, and when speaking of conductance we refer to a parallel equivalent circuit

*It is convenient to use the term "field emission" in those cases when the cathode emission depends strongly on the intensity of the electric field at its surface In particular, this may be cold emission, the Schottky effect in vacuum diodes, the Zener effect, impact ionization in semiconductor diodes, or others.

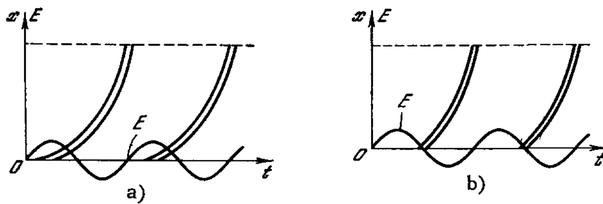

FIG. 3. Space-time diagram of electron motion in a "field emission" diode, a) without emission delay, b) with emission delay.

to the extent of completely suppressing the self-oscillations. Moreover, under certain conditions this feedback may turn out to be sufficient to cause self-oscillations in the circuit, without any need for an external high-Q tank circuit at all. In such a case the diode gap operates as a self-oscillating system, producing in an external active load current pulses of a frequency determined by the delay time and by the "operating" speed of the negative feedback.

The foregoing considerations are general and are applicable not only to vacuum-tube diodes but also to diodes of other types - dielectric, semiconductor, etc., with due allowance, of course, for the specific nature of the carrier motion in solids. In particular, these considerations have a direct bearing on the operating mechanism of the avalanche-transit diodes.

Whereas semiconductor diodes with "drooping" static voltage-current characteristics have been known for more than 40 years (the first such diode was the crystadyne of O. Losev [12]), and different variants of such devices have been under investigation since that time, the idea of producing semiconductor analogs of vacuum-tube diodes with dynamic negative resistance has occurred relatively recently.

In general form, this idea was formulated in a paper by Schockley [13], who also proposed several variants of p-n diodes in which the negative dynamic resistance is the result of transit effects accompanying the diffusion and drift of the minority carriers in a thin layer of n-type semiconductor under the influence of an electric field.

The most interesting among the subsequent researches in this direction is the theoretical work by Read [14]. He proposed a variant of semiconductor diode with dynamic negative resistance for microwave frequencies, based on the use of the impact ionization effect in an inversely biased n-p junction,

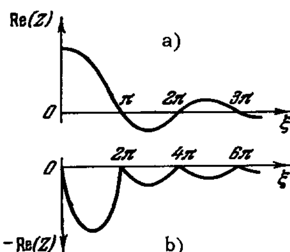

FIG 4. Active resistance of field-emission diode, a) without emission delay, b) with emission delay.

to obtain a carrier flux interaction with a high-frequency field in some transit space. According to Read, the transit space should be the depletion layer of an i-semiconductor following the n-p junction, so that the diode should have an n^+-p-i-p^+ structure and should operate under conditions of breakdown through the i-layer.

Practical realization of such a model (the Read diode) met with considerable technological difficulties, and this caused a considerable lag in experimental research in this direction [15-16]. Nonetheless, Read's basic idea, that of combining transit effects with impact ionization, is correct and is applicable to a much broader class of diode structures, including avalanche-transit p-n diodes (ATD).

Unlike the Read diode, which can be called a p-i-n ATD, in the p-n ATD the transit space is part of the barrier layer of the usual p-n junction, and the question of the character of the distribution of the impurity atoms in a direction normal to the p-n junction plane is not fundamental. The negative dynamic resistance can be obtained in diodes with stepwise and with smooth p-n junctions. or in diodes with p-n junctions of other types. All that matters is the volume character of the breakdown. In this sense, the occurrence of negative dynamic resistance in the impact ionization mode is a property of any ideal p-n junction.

The operation of the p-n ATD can be represented schematically as follows: Let us consider an inversely biased planar p-n junction (Fig. 5). When the inverse bias V increases, the electric field intensity E in the barrier layer increases, reaching at $V = V_{br}$ a value $E_{br} \simeq 10^5$ V/cm, at which intense impact ionization of the crystal atoms by the mobile carriers begins and leads to avalanche-like multiplication of the number of carriers and to the creation of new electron-hole pairs.

Since the probability of impact ionization is a very rapidly increasing function of the electric field intensity, the region where carrier creation takes place is confined to a more or less narrow layer in which the field is maximal, the so-called multiplication layer. The holes and electrons produced in the layer under the influence of a strong electric field drift through the p and n transit sections of the barrier layer (Fig. 5) with practically constant velocities v_p and v_n.*

Thus, an inversely biased p-n junction at a voltage close to breakdown constitutes a diode gap in which the role of the cathode is played by the multiplication layer, and the role of the transit space by the remainder of the barrier layer. The emission of such a

*When $E > 10^3$ V/cm, the carrier velocities, limited by scattering by optical phonons, increase little with increasing field, we can assume approximately that $v_p \approx v_n \approx 6 \times 10^6$ cm/sec in Ge and $v_p \approx v_n \approx (0\ 8 - 1) \times 10^7$ cm/sec in Si

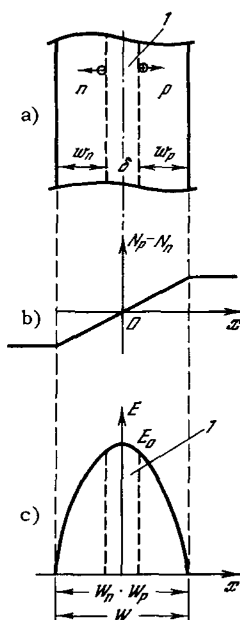

FIG. 5. Diagram of gradual symmetrical p-n junction of ATD, a) barrier layer, b) distribution of impurity ions, c) variation of electric field; 1 – multiplication layer.

cathode has a clearly pronounced "field" character, in that the current leaving the multiplication layer increases or decreases with the electric field intensity in this layer. The avalanche nature of the emission current causes its inertial properties, since a definite time is required for the avalanche to develop, so that the instantaneous value of the electric field determines not the value of the avalanche current itself, but only its rate of change in time. Therefore the change in the current does not follow instantaneously the change in the electric field, but lags it in phase by an amount close to $\pi/2$.

Such a p-n junction is very similar in its properties to the optimal variant of the field diode, in which the emission current lags the field by one quarter of a cycle, as shown on the space-time diagram in Fig. 4b. Therefore the main deductions made above regarding the properties of the field diode with delayed emission are applicable also to the avalanche-transit diode. This pertains, in particular, to the considerations of the delayed action of the space charge of the mobile carriers on the avalanche current, which greatly facilitates the self excitation of a generator with ATD.

At the same time, the ATD has some unique features connected with the avalanche nature of the current, of which one is fundamental. Owing to the finite width of the multiplication layer, the phase shift between the field and the current in this layer exceeds $\pi/2$, and the multiplication layer itself has negative resistance. In most practically realized diode structures, this effect is secondary, but under special operating conditions its role may become significant.

Besides the avalanche-transit diode, there can obviously exist other semiconductor diodes with dynamic negative resistance. In principle, for example, an inversely biased p-n junction in which the breakdown is connected not with impact ionization but with the Zener effect (tunnel effect), should also possess this property. However, the practically inertialess nature of the tunnel effect at frequencies lower than 10^{12} Hz makes this diode much less convenient for microwave generation than the ATD.

A theoretical analysis of the Read diode is the subject of two papers [14,19] in which a very simple diode model is considered, consisting of a narrow p-n junction with stepwise distribution of the impurity, and an extended i-layer. It is assumed that the entire impact ionization is concentrated in the p-n junction plane, in a layer of negligibly small arbitrarily specified thickness δ, which enters into the final equations as one of the main independent parameters.

In [19] the analysis is confined to the high-frequency properties of the diode in the linear approximation, while in [14] an estimate of the nonlinear properties of the diode is also presented, and certain factors limiting the efficiency and the output of a Read-diode generator are considered. A more general approach, which takes into account the real distribution of the intensity of impact ionization in a diode with arbitrary impurity distribution, was developed, as applied to p-n ATD, in a paper by the author [3], in unpublished papers by A. L. Zakharov, who considered both linear and nonlinear theories of ATD, and also in a recent paper by T. Misawa [20]. In this analysis the Read model is considered as a particular case. We shall therefore follow the cited papers in the exposition that follows.

3. STATIC VOLTAGE-CURRENT CHARACTERISTIC AND DIFFERENTIAL RESISTANCE OF THE ATD IN THE AVALANCHE BREAKDOWN MODE

In the static mode, when $|V| > V_{br}$, the current through the diode is limited by the space charge of the majority carriers, electrons and holes, which flow respectively through the n and p regions of the barrier layer in the p-n ATD or through the i-region of the p-i-n ATD. The electric field distribution in these regions is determined by the Poisson equation

$$\frac{dE}{dx} = \frac{e}{\varepsilon}\left(N_n - N_p + \frac{\mathcal{J}_p}{ev_p} - \frac{\mathcal{J}_n}{ev_n}\right), \tag{3.1}$$

where N_p and N_n are the densities of the acceptors and donors respectively, e the absolute value of the electron charge, ϵ the dielectric constant of the semiconductor, $\mathcal{J}_p = epv_p$ and $\mathcal{J}_n = env_n$ are the hole and electron current densities (we neglect diffusion), and p, n, and $v_{p,n}$ are their densities and velocities; we shall henceforth put $v_p = v_n = v$.

To clarify the fundamental relations, let us consider first a simplified p-n junction model, in which the carrier source is localized in an infinitesimally narrow layer in the contact plane between semicon-

ductors having different types of conductivity. We assume that the carrier emission from this layer can be regarded as unlimited when the electric field intensity in the layer, E_0, is equal to the breakdown value, E_{br}. In this case the current flowing through the p-n junction, with density $\mathcal{J}$, is transferred into the p-region only by the holes, and into the n-region only by the electrons, so that $\mathcal{J}_p = \mathcal{J}_n = \mathcal{J}$, and the integration of (3.1) with respect to x and over the area of the p-n junction yields directly the voltage-current characteristic and the differential resistance R_0 of the p-n junction.

Thus, for example, for an abrupt p-n junction with a stepwise impurity distribution ($N_n - N_p$ = const) we obtain directly

$$V=\frac{1}{2}E_{br}\sum_{j=p,n}\frac{W_j}{1-\frac{i}{(i_m)_j}}, \quad (3.2)$$

$$R_0=\frac{1}{2v}\sum_{j=p,n}\frac{W_j}{C_j}\frac{1}{1-\frac{i}{(i_m)_j}}, \quad (3.3)$$

where $i = \mathcal{J}S$ is the total current of the diode, $i_m = \mathcal{J}_m S$, $(\mathcal{J}_m)_j = eN_j v$ is the limiting current density at which the space charge of the carrier neutralizes the space charge of the impurity, and $C_j = \epsilon S/W_j$ is the capacitance of the j-th section of the barrier layer of width W_j; the values of all quantities are taken at $V = V_{br}$.

The voltage-current characteristic of the diode i(V) determined by expression (3.2) is shown in Fig. 6 by the dashed line. When $i/i_m \ll 1$, i(V) is nearly linear with a constant differential resistance

$$R_0=\frac{1}{2}\sum_{j=p,n}\frac{W_j}{vC_j}. \quad (3.4)$$

As $i \to i_m$, the barrier layer rapidly broadens with increasing current, and the resistance R_0 grows sharply. However, at ordinary impurity concentrations the values of the limiting current density $\mathcal{J}_m$ are quite large, for example $\mathcal{J}_m \simeq 10^4$ A/cm^2 for $N = 10^{16}$ cm^{-3}, therefore for the greater part of the voltage-current characteristic the differential resistance of the p-n junction is close to that given by (3.4) and does not depend on the current.

The resistance (3.4) has a simple physical meaning: If the source of the mobile carriers has at $V > V_{br}$ an unlimited emission, then the increment $\Delta V = V - V_{br}$ of the potential difference is compensated by the space-charge field of the mobile carriers, which are uniformly distributed over the entire width W of the p-n junction, $\Delta V = \mathcal{J}W^2/2\epsilon v$, corresponding to (3.4).

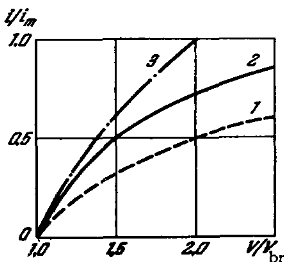

FIG. 6. Static voltage-current characteristics of ATD. 1 – Localized multiplication layer, 2 – abrupt p-n junction, 3 – gradual p-n junction.

Real avalanche-transit diodes differ from the foregoing simple model first, in that the source of the mobile carriers is "smeared" over the volume of the barrier layer and, second, in that the rate of production of new carriers depends on the electric field intensity. To calculate the voltage-current characteristic in this case it is necessary to add to the Poisson equation the continuity equations

$$-\frac{d\mathcal{J}_n}{dx}=\alpha\mathcal{J}_n+\beta\mathcal{J}_p, \qquad \frac{d\mathcal{J}_p}{dx}=\beta\mathcal{J}_p+\alpha\mathcal{J}_n \quad (3.5)$$

and the breakdown condition. In (3.5) α and β are the coefficients of impact ionization for electrons and holes, which are equal to the number of pairs produced by these carriers per unit length. In germanium and in silicon, the coefficients α and β are connected by the approximate relation $\beta = k\alpha$ ($k \simeq 2$ for germanium and $k \simeq 1/10$ for silicon), and the breakdown condition takes the simple form [21]

$$\int_{-W_n}^{W_p}\bar{\alpha}\,dx=1-\frac{i_s}{i}, \quad (3.6)$$

where $\bar{\alpha} = (k-1)\alpha/\ln k$, and i_s is the minority-carrier current (saturation current).

The voltage-current characteristic of an abrupt p-n junction in the region $i \gg i_s$, obtained by simultaneously solving Eqs. (3.1), (3.5), and (3.6) under the assumption of a power-law dependence of the coefficients α and β on the field, $\beta \sim \alpha \sim \bar{\alpha} \sim E^n$ ($n = 5.5$), is shown in Fig. 6 by the solid line. It is qualitatively similar to the characteristic calculated in elementary fashion. The voltage-current characteristic of a gradual p-n junction with linear impurity distribution has a similar form (Fig. 6). When $i/i_m \ll 1$, the electric field distribution in the p-n junction does not vary with the current, and the voltage-current characteristic is linear in both cases.* However, the differential resistance of the p-n junction differs in this section from (3.4) by a factor $\rho < 1$, which depends (for a specified form of the function $\bar{\alpha}(E)$) on the impurity distribution in the p-n junction. For an abrupt p-n junction with a linear field distribution in the barrier layer, this factor is $\rho_1 \simeq 0.62$, and for a gradual p-n junction with parabolic field variation we have $\rho = \rho_2 \simeq 0.43$. Thus, the smoother the variation of the field near the maximum value, i.e., the broader the section in which the probability of impact ionization differs from zero, the smaller the factor ρ. This is to be expected, since in this section the current is carried both by electrons and holes, whose space

*For a gradual p-n junction with linear impurity gradient M cm^{-4}, the limiting current can be expressed as $\mathcal{J}_m = eMvW$

charges partially cancel each other. The more uniformly the multiplication is distributed over the width of the p-n junction, the smaller the space charge of the mobile carriers for a specified current, and consequently, the smaller the differential resistance of the p-n junction.

The indicated simple connection between the rigorous calculation of the differential resistance and the elementary relation (3.4) enables us to introduce the concept of the "equivalent multiplication layer"*, which is defined as the section in which the total avalanche current i_0 is generated and in which the space charge is equal to zero. The width of the equivalent multiplication δ can be obtained from the relation

$$2R_0 = \rho \sum_{j=p,\,n} \frac{W_j^2}{\varepsilon v S} = \sum_{j=p,\,n} \frac{(W_j - \delta_j)^2}{\varepsilon v S}, \tag{3.7}$$

hence

$$\frac{\delta_j}{W_j} = \frac{\delta}{W} = 1 - \sqrt{\rho} \quad (\delta = \delta_p + \delta_n,\ W = W_p + W_n).$$

For abrupt and continuous p-n junctions in germanium or silicon we have respectively $\delta/W = 0.21$ and $\delta/W = 0.35$, i.e., the multiplication layer is an appreciable fraction of the entire barrier layer.

If the breakdown encompasses the entire area S of the p-n junction then, in accord with (3.4) and (3.7), the product R_0C does not depend on S or (when $i \ll i_m$) on the distribution of the current in this area, and is a single-valued function of the breakdown voltage V_{br}. For a gradual symmetrical p-n junction ($W_p = W_n$) in germanium, for example, $R_0C = 0.43\ W/4v \simeq 6 \times 10^{-14}\ V_{br}$.

4. HIGH-FREQUENCY CHARACTERISTICS OF ATD. FUNDAMENTAL RELATIONS

In a rigorous analysis of high-frequency processes in an ATD it is necessary to start from the nonstationary kinetic equation for the electrons and holes, and solve it simultaneously with the equation of the electromagnetic field in the crystal. In such a formulation, however, this problem can hardly be solved in general form. It becomes necessary therefore to introduce in the analysis, at the very outset, a number of more or less fundamental assumptions.

The analysis is confined to the region of not too high frequencies, when the time of Maxwellian relaxation and the free-path time of the carriers can be neglected compared with the period of the oscillations, and the multiplication process can be regarded as quasistationary, assuming the ionization probability to be a single-valued function of the electric field intensity and not to depend explicitly on the coordinates and the time. The p-n junction is assumed planar, with dimensions much smaller than the wavelength of the oscillations in the crystal. As a rule, these assumptions are satisfied up to frequencies of the order of 10^{11} Hz, corresponding to the shortwave part of the millimeter band.

Under these conditions, the kinetic equations for the electrons and holes reduce to the continuity equations

$$\begin{aligned} e\frac{\partial p}{\partial t} &= -\frac{\partial \mathcal{J}_p}{\partial x} + \alpha \mathcal{J}_n + \beta \mathcal{J}_p, \\ e\frac{\partial n}{\partial t} &= \frac{\partial \mathcal{J}_n}{\partial x} + \alpha \mathcal{J}_n + \beta \mathcal{J}_p, \end{aligned} \tag{4.1}$$

which must be solved simultaneously with the Poisson equation (3.1) and the equation for the total current

$$\varepsilon \frac{\partial E_{(x,\,t)}}{\partial t} + \mathcal{J}_e(x, t) = \mathcal{J}(t), \tag{4.2}$$

where $\mathcal{J}(t)$ is the density of the total current, which in a planar diode does not depend on the coordinates x; $\mathcal{J}_e = \mathcal{J}_p + \mathcal{J}_n$ is the conduction-current density. Since $\alpha = \alpha(E)$ and $\beta = \beta(E)$, the system of equations (3.1), (4.1), and (4.2) is nonlinear and cannot be solved analytically. Moreover, it is impossible to obtain an analytic solution in general form even after these equations are linearized with respect to small time changes of all the quantities. The problem must therefore be simplified further.

Let us assume, for example, that the transit angle of the carriers in the multiplication layer is sufficiently small ($\omega\delta/2v < 1$), so that the variation of the field and of the current in this layer within the time $\tau_\delta = \delta/2v$ can be neglected. Furthermore, to simplify the derivations, we put $\alpha = \beta = \overline{\alpha}$.

In this case the processes in the multiplication layer can be regarded in the quasistatic approximation, using the concept of the equivalent multiplication layer in the form introduced above. The barrier layer of p-n junction is then subdivided into three regions: the multiplication layer, in which all the multiplication is concentrated, and two carrier-drift regions (transit sections), in which there is no multiplication. In the equivalent multiplication layer, the electron and hole densities are equal and the total space-charge density of the mobile carriers is equal to zero. The total multiplication current $i_e(t, \delta_{n,p}) = i_0(t)$ flows from the boundaries of this layer into the drift region, being completely transported by holes in a p-type semiconductor and by electrons in an n-type semiconductor. Such a carrier distribution is obviously realized if the electron-hole pairs are generated on the boundaries of the equivalent multiplication layer. Therefore the width δ of this layer is none other than the mean free path between the ionizing collisions, and the quantity $\tau_\delta^{-1} = v/\delta$ is the ionization probability.

The use of such a simple model greatly facilitates the calculations, the results of which turn out to be equally applicable to p-n and to p-i-n ATD at not too high frequencies.

*This concept was first introduced by A. L. Zakharov on the basis of an analysis of the high-frequency properties of the multiplication layer

The two continuity equations (4.1) and (4.2) are replaced by a single equation for the current i_0 flowing out of the equivalent multiplication layer. This equation can be obtained by integrating (4.1) with respect to x with allowance for conditions on the p-n junction boundary [14,19]

$$i_p\Big|_{-W_n} = i_{ps},\quad i_n\Big|_{-W_n} = i - i_{ps},\quad i_p\Big|^{W_p} = i - i_{ns},\quad i_n\Big|^{W_p} = i_{ns},$$

where i_{ps} and i_{ns} are respectively the hole and electron components of the saturation current.

As a result we obtain

$$\tau_\delta \frac{di_0}{dt} = 2i_0\,[\Psi(E_0) - 1] + 2i_s, \tag{4.3}$$

where

$$\Psi(E_0) = \int\limits_{-W_n}^{W_p} \bar{\alpha}(E)\,dx \tag{4.4}$$

is the integral multiplication in the barrier layer. In the quasistatic approximation considered above, $\Psi(E_0)$ can be calculated by using the relation for $E(x)$ obtained for the p-n junction in the absence of the current; with this, $\Psi(E_0) = (E_0/E_{br})^{n+l}$, where $l = 1$ for an abrupt p-n junction and $l = 1/2$ for a gradual one [14].

As shown by a more detailed analysis*, the amplitude relations between the current and the field are determined by (4.3) with an error smaller than $(\omega\tau_\delta/2)^2$, and the phase relations with an error of the order of $\omega\tau_\delta$. The latter error is more significant, but it can be corrected for by introducing into (4.3) a time shift τ_γ between E_0 and i:

$$\frac{\tau_\delta}{2}\frac{di_0(t)}{dt} = i_0(t)\,\{\Psi\,[E_0(t+\tau_\gamma)] - 1\} + i_s. \tag{4.5}$$

The parameter τ_γ depends on the amplitude of the oscillations and the distribution of the impurity in the p-n junction. It is important that under ordinary impurity distributions this parameter is negative and its value is the larger, the more uniform the multiplication distribution over the entire layer. Thus, for example $\tau_\gamma = -0.0007\tau$ for an abrupt p-n junction and $\tau_\gamma = -0.055\tau$ for a continuous one $(\tau = (W - \delta)/2v)$.

The Small-Amplitude Approximation

For a given $\Psi(E_0)$ dependence, the system of equations (3.1), (4.2), and (4.5) determines, in principle, the connection between the voltage V applied to the diode and the current i flowing through it.

This connection can be readily obtained in explicit form for small amplitudes of the high-frequency signal, when the indicated equations can be linearized with respect to small alternating components of the current $\tilde{i}(t)$, of the field $\tilde{E}_0(t)$, and the voltage $\tilde{V}(t)$, which are assumed proportional to $\exp(j\omega t)$.

*This analysis was made by A. L. Zakharov [42].

As a result we obtain

$$\tilde{i}_0(t) = \frac{S}{j\omega L_\delta}\tilde{E}_0(t') + ja\tilde{i}_0(t), \tag{4.6}$$

$$\tilde{i}(t) - \tilde{i}_0(t) = j\omega\varepsilon S\tilde{E}_0(t), \tag{4.7}$$

$$\frac{S}{L_\delta}\tilde{E}_0(t') = \Omega^2\Big[CV(t) + \frac{1}{2}\sum_{j=p,n}\frac{v}{W_j}\int\limits_{t'-\tau_j}^{t'} i_0(u) \times (u + \tau_j - t')\,du\Big], \tag{4.8}$$

where $a = (2/\omega\tau_\delta)(i_s/i^0)$, $i^0 = S\mathcal{J}^0$ is the dc component of the diode current, and

$$t' = t + \tau_\gamma,\quad 2\tau = \tau_p + \tau_n,\quad \tau_{p,n} = \frac{W_{p,n} - \delta_{p,n}}{v} = \frac{w_{p,n}}{v},$$

$$L_\delta = \frac{\tau_\delta}{2\mathcal{J}^0\left(\dfrac{\partial\Psi}{\partial E}\right)_{E_{br}}},\quad \Omega = (L_\delta\varepsilon)^{-\frac{1}{2}} = \left[\frac{2\mathcal{J}^0\left(\dfrac{\partial\Psi}{\partial E}\right)_{E_{br}}}{\tau_\delta\varepsilon}\right]^{\frac{1}{2}}$$

and the specific inductance and the proper characteristic frequency of the multiplication layer, which characterize (together with τ_γ) the inertia and the oscillatory properties of the avalanche development process.

The main consequence of Eq. (4.5) is that the current $i_0(t)$ flowing out of the multiplication layer lags the field $E_0(t)$ in this layer. In the linear approximation, according to (4.6), the connection between these quantities is close to inductive, so that for sinusoidal signals the phase shift between $i_0(t)$ and $E_0(t)$ is approximately equal to $\pi/2$. This makes it possible to classify the ATD as field diodes with delayed emission, which, as indicated in Sec. 2, are the most effective among the active diode elements.

The high-frequency properties of the ATD depend on the characteristic frequency Ω, which determines the rate of change of the field E_0 and of the current i_0 in the multiplication layer. In particular, the resistance of the layer at a small signal can be negative only at sufficiently high frequencies $\omega > \Omega$. This can be verified by considering the phase relations between the currents and the voltage in the p-n junction. We neglect first the small quantities $\omega\tau_\gamma \ll 1$ and $a \ll 1$. It then follows from (4.6) that the conduction current $\tilde{i}_0 = S\tilde{E}_0/j\omega L_\delta$ is opposite in phase to the displacement current $\tilde{i}_d = j\omega\varepsilon S\tilde{E}_0$, and the ratio of their magnitudes is $\Omega^2/\omega^2 = \beta^2$. The conduction current lags the field $\tilde{E}_0(t)$ in phase by $\pi/2$, and the displacement

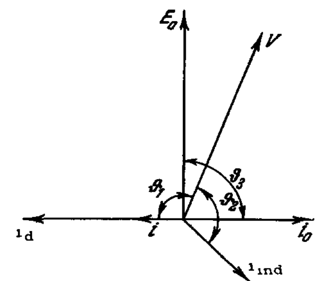

FIG. 7. Vector diagram of the currents and voltages in the ATD p-n junction.

current leads it. On the other hand, Eq. (4.8) shows that under the influence of the carrier space charge in the transit sections (the second term in the right side of (4.8)), the voltage $\tilde{V}(t)$ applied to the p-n junction always lags in phase the field in the multiplication layer $\tilde{E}_0(t)$. Consequently the phase shift between $\tilde{V}(t)$ and $\tilde{i}_0(t)$ is always smaller than $\pi/2$, and that between $\tilde{V}(t)$ and $\tilde{i}_d(t)$ is larger than $\pi/2$ (see the vector diagram of Fig. 7). The active resistance of the p-n junction is negative if the phase shift ϑ_1 between $\tilde{V}(t)$ and the total current $\tilde{I}(t)$ is larger than $\pi/2$. Inasmuch as the phase of the current $\tilde{I}(t)$ coincides with the phase of the larger of the quantities $\tilde{i}_0(t)$ or $\tilde{i}_d(t)$, this condition is satisfied when $|\tilde{i}_d| > |\tilde{i}_0|$, i.e., when

$$\beta^2 < 1. \tag{4.9}$$

The same conclusions can be arrived at by determining the phase shift ϑ_2 between the voltage $\tilde{V}(t)$ and the current $\tilde{i}_{ind}(t)$ induced in the external circuit by the mobile carriers (Fig. 7). The requirement $\vartheta_2 > \pi/2$ also leads to condition (4.9). In the general case when $\tau_\gamma \neq 0$ and $a \neq 0$, the current $\tilde{i}_0(t)$ lags the field $E_0(t)$ not by $\pi/2$, but by the angle

$$\vartheta_3 = \frac{\pi}{2} - \operatorname{arctg}\sigma, \quad \sigma = \omega\tau_\gamma + a.$$

The phase shift between $\tilde{V}(t)$ and $\tilde{E}_0(t)$ also depends on σ, and the condition (4.9) is replaced by $\beta^2 < 1 - \sigma U(\xi_p, \xi_n)$, where $U(\xi_p, \xi_n)$ is a certain function of the transit angles $\xi_{p,n} = \omega\tau_{p,n}$. Usually, however, $\sigma \ll 1$ and this condition differs little from (4.9).

It is often convenient to use, besides the characteristic frequency, a second parameter - the characteristic current i_x, defined at the frequency ω by

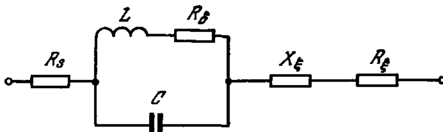

FIG. 8. Equivalent circuit of ATD.

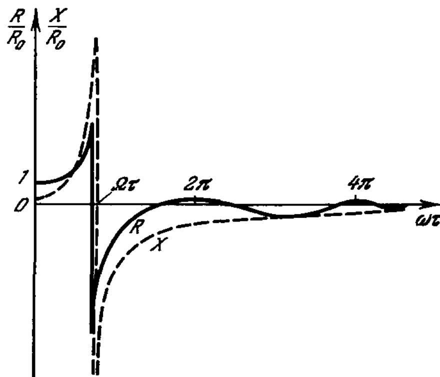

FIG. 9. Schematic dependence of the resistance and reactance of the ATD on the frequency.

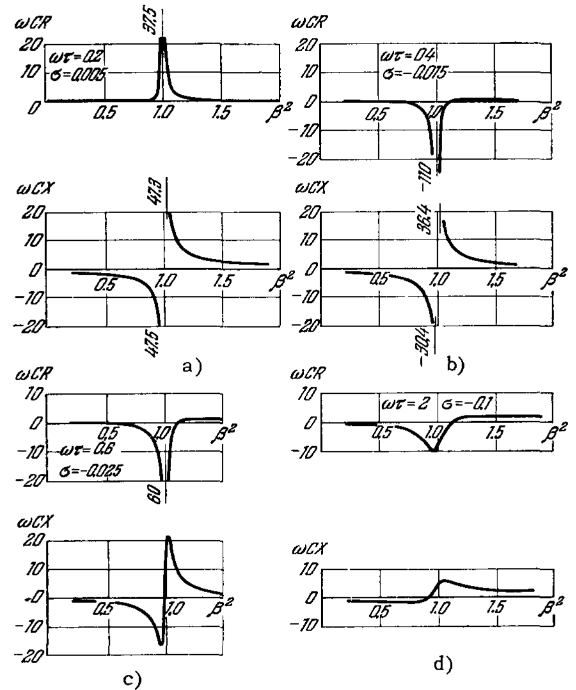

FIG. 10. Resistance and reactance of a symmetrical ATD p-n junction vs. diode current for different values of the transit angle.

the condition $\Omega(i^0) = \Omega(i_x) = \omega$. Then $\beta^2 = i^0/i_x$.

The impedance of the p-n junction of the ATD in the linear mode, $Z = \tilde{V}/\tilde{i}$, is obtained by eliminating $\tilde{i}_0$ and $\tilde{E}_0$ from (4.6)—(4.8):

$$Z(\omega) = R(\omega) + jX(\omega),$$

$$\omega CR = \omega C(R_\delta + R_\xi) = \frac{\sigma\beta^2}{(1-\beta^2)^2+\sigma^2} - \frac{\beta^2}{(1-\beta^2)^2+\sigma^2} \sum_{j=p,n} \frac{C}{C_j'} [(1-\beta^2)\chi(\xi_j) + \sigma\mu(\xi_j)],$$

$$\omega CX = \omega C(X_\delta + X_\xi) = -\frac{1-\beta^2}{(1-\beta^2)^2+\sigma^2} + \frac{\beta^2}{(1-\beta^2)^2+\sigma^2} \sum_{j=p,n} \frac{C}{C_j'} [(1-\beta^2)\mu(\xi_j) - \sigma\cdot\chi(\xi_j)], \tag{4.10}$$

where $C_j' = S\epsilon/w_j$ is the capacitance of the j-th transit section

$$\chi(\xi) = \frac{1-\cos\xi}{\xi}, \qquad \mu(\xi) = 1 - \frac{\sin\xi}{\xi}.$$

The expressions in (4.10) correspond to the equivalent ATD circuit shown in Fig. 8.

In this circuit, the LCR_δ loop takes into account the "cold" capacitance $C = S\epsilon/W$ of the p-n junction and the parameters $L = L_\delta W$ and $R_\delta = \sigma\omega L$ of the multiplication layer. The quantities R_ξ and X_ξ pertain to the transit sections, and the resistance R_s characterizes the loss in the diode base.

The dependence of the resistance R and of the reactance X of the ATD p-n junction on the frequency is shown in Fig. 9. The dependence of R and X on the diode current for a symmetrical p-n junction, as calculated from formulas (4.10) for several values of

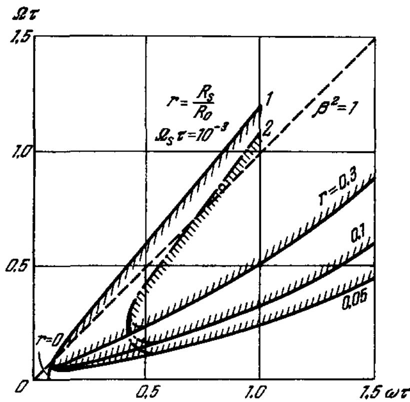

FIG. 11. The region of negative resistances of the ATD is bounded by the curves: 1 – without allowance for the inhomogeneity of the breakdown, 2 – with allowance for the inhomogeneity of the breakdown.

the frequency and the working interval $\omega\tau < 2\pi$, is shown in Fig. 10.

According to (4.10), at small amplitudes of the high-frequency signal the impedance of the ATD p-n junction at the frequency ω is determined essentially by the carrier transit angles $\xi_{p,n}$ in the transit sections of the barrier layer of the p-n junction, and by the parameter $\beta^2 = \Omega^2/\omega^2 = i^0/i_x$. The reactance of the p-n junction, which is inductive at low frequencies, reverses sign and becomes capacitive when $\beta^2 \simeq 1$, approaching $-(\omega C)^{-1}$ as $\beta^2 \to 0$.

The resistance of the p-n junction coincides at low frequencies* with its differential resistance R_0 and remains positive up to a frequency somewhat lower than the characteristic frequency ($\beta^2 \lesssim 1 - \sigma$), where it reverses sign and reaches the maximum negative value. With further increase in frequency, the resistance of the p-n junction remains negative, but its magnitude decreases rapidly (approximately like ω^{-3}), assuming a minimum value at $\xi_{p,n} \simeq 2\pi n$.

Thus, the active resistance of the diode $R_d = R + R_s$ is negative in some range of frequencies and currents, defined by the condition $\beta^2_{min} < \beta^2 < 1$, where β^2_{min} depends on the loss resistance R_s. For not too high frequencies ($\omega\tau < 2\pi$) the region of negative values of R is shown in Fig. 11 (shaded), the dashed curve corresponding to the characteristic current $i_x(\omega)$. The lower limit ω_{min} of the frequency range where $R < 0$ is determined by the value of the parameter σ, i.e. (when $\omega\tau \ll 1$), by the value of the saturation current i_s: $\omega_{min}\tau \simeq 2(\Omega_s\tau)^{1/2}$, $\Omega_s = \Omega(i_s)$. The curves $r = R_s/R_0 = \text{const}$ in this figure define the starting current of the diode i_{st}, below which $R_d > 0$. The inhomogeneity of the p-n junction, which leads to a nonuniform development of the breakdown over its area, narrows down the region where $R_d < 0$, as shown by the dash-dot lines in Fig. 11.

Inside the indicated region, the absolute value of the negative resistance of the diode increases rapidly as the current increases, and approaches its characteristic value ($\beta^2 \to 1$) (Fig. 10). This effect, which is due to the retarding action of the space charge of the mobile carriers on the field in the multiplication layer, ensures not only large values of negative resistance of the diode, but also low values of its negative $Q = \omega \frac{\partial X}{\partial \omega}/R$, the modulus of which can be of the order of unity in a certain interval of frequencies or currents near $\beta^2 \simeq 1$ [3,20]. This greatly facilitates the excitation of the self oscillations in a generator using an ATD, and relaxes the requirements with regards to the Q of the diode ($Q_s = (\omega C R_s)^{-1}$) and the external resonator. Moreover, if $\sigma < 0$, then $R < 0$ with $X = 0$ (see Figs. 10 and 11). This points to the possible self excitation in the ATD of internal self-oscillations that are weakly coupled with the external circuit and whose frequency at $|\sigma| \ll 1$ is close to the characteristic frequency.

Although in ordinary p-n ATD the latter effect does not play a major role, owing to the smallness of τ_γ and σ, it is of fundamental significance, since it reflects the instability of the impact-ionization process itself. As follows from the foregoing (see Fig. 7), this instability is connected with the fact that when $\sigma < 0$ the phase shift ϑ_3 between the field and the conduction current in the multiplication layer exceeds $\pi/2$.

To clarify this, let us consider a broad multiplication layer (Fig. 12) and let us estimate the phase shift between the alternating field $E(t)$ and the carrier flux $\tilde{p}(t)$ generated by this field, which for concreteness we assume to be holes. The rate of hole generation, which is proportional to the product $\bar{\alpha}(E)p$, depends on the value of the field E and on the hole density p. Since the change in the density $\tilde{p}(t)$ lags in phase the variation of the field $\tilde{E}(t)$, the generation rate will also lag the field in phase. But the phase shift between $\tilde{p}(t)$ and $d\tilde{p}(t)/dt$ is $\pi/2$. Therefore the phase shift between $\tilde{p}(t)$ and $\tilde{E}(t)$, and consequently between $\tilde{i}_p(t)$ and $\tilde{E}(t)$ is larger than $\pi/2$. A similar result is obtained also for the electron current $i_n(t)$ and the conduction current $i_e(t) = i_n(t) + i_p(t)$. A consequence of this fact is the high-frequency instability of the impact ionization process, which becomes manifest, on the one hand, in

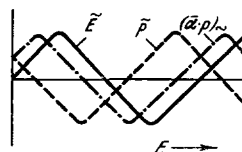

FIG. 12. Illustrating the analysis of the instability in the multiplication layer.

*By low frequencies are meant here those lying below the microwave band, but exceeding 0.5 – 1 MHz. At lower frequencies the differential resistance of the ATD differs from (3.7), owing to the therma. inertia of the diode (see Sec. 7).

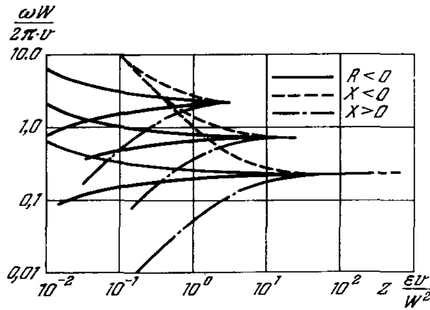

FIG. 13. Resistance and reactance of the multiplication layer in the case of homogeneous ionization ($\bar{\alpha}$ = const).

an exponential growth (in time) of small perturbations of the electric field and of the carrier density in the multiplication layer, and on the other hand in a negative value of its active resistance R_δ.

It must be emphasized that these conclusions are valid also for a broad multiplication layer, for which the previously-assumed condition $\omega\tau_\delta/2 < 1$ is not satisfied. An analytic result could be obtained in this case only for one highly idealized model - a layer with uniform distribution of the multiplication ($\bar{\alpha}$ = const). However, numerical calculations carried out in the linear approximation for more realistic models have confirmed the correctness of the basic analytic relations [20].

The impedance of such a multiplication layer, calculated without allowance for the saturation current in the aforementioned idealized model, is shown in Fig. 13. The parameter on the curves is the dc density relative to 1.4×10^3 A/cm^2. As shown by this figure, the resistance of the multiplication layer is negative also at angles $\omega\tau \gtrsim 2\pi$. However, the current densities required for this purpose are quite high.

Characteristics of ATD at Large High-frequency Signal Amplitudes

A rigorous analysis of the initial system of nonstationary ATD equations (3.1), (4.1)—(4.2) for arbitrary values of the variables leads to exceedingly cumbersome calculations, even if numerical methods are used. The main features of the nonlinear ATD characteristics can be established, however, by a semi-analytic method, by introducing in sequence a number of supplementary simplifications. We neglect the modulation of the p-n junction width and of the multiplication-layer parameters by the alternating voltage, and assume that either this voltage or the alternating current in the external circuit are sinusoidal functions of the time. The latter assumptions are valid, in particular, when the diode is connected to a resonator with sufficiently high Q and the condition $\beta^2 \ll 1$ is satisfied at the operating frequency ($\beta^2 < 0.5$ is sufficient in practice). Under these assumptions, the main features of the high-frequency ATD characteristics at large oscillation amplitudes are determined by two nonlinear effects: the nonlinear dependence of the avalanche current and the space-charge produced by it on the integral multiplication $\Psi(E_0)$, and the nonlinearity of the function $\Psi(E_0)$, which can be called respectively the current nonlinearity and the multiplication nonlinearity. Let us explain the role of each of the foregoing nonlinear mechanisms by means of very simple models.

a) Current nonlinearity. We neglect the multiplication nonlinearity, expanding the function $\Psi(E_0)$ in the avalanche equation (4.5) in powers of $\tilde{E}_0/E_{br}$ and neglecting the terms proportional to the second and higher powers of this ratio. Eliminating $\tilde{E}_0$ from the obtained equation and from (4.2), and putting $i_s = \tau_\gamma = 0$, we arrive at the equation

$$\frac{d^2 \ln i_0(t)}{dt^2} = \frac{\Omega^2 [i(t) - i_0(t)]}{i^0}. \qquad (4.11)$$

We assume further that the current $i(t)$ in the external circuit varies sinusoidally: $i(t) = i^0 + i_1 \cos \omega t$, and neglect in the right side of (4.11) the conduction current $i_0(t)$ compared with the total current $i(t)$, which is equivalent to the condition $\beta^2 \ll 1$ and $i_1 \simeq (i_d)_1 = \omega C V_1$, where V_1 is the amplitude of the first harmonic of the voltage $V(t)$. The solution of the obtained equation under the initial conditions $t = 0$, $i_0 = i_{00}$, and $di_0/dt = 0$ has the following simple form:

$$i_0(\omega t) = i_{00} \exp[z(1 - \cos \omega t)], \qquad (4.12)$$

where $z = \beta^2(i_1/i^0) = i_1/i_x \simeq \omega C V_1/i_x$.

According to (4.12) and Fig. 14, the avalanche current $i_0(t)$ becomes a strongly nonsinusoidal function of the time even at relatively small values of the parameter z ($z > 0.5$), corresponding to small values of the alternating-signal amplitude $V_1/V_{br} \simeq 0.1\ \omega\tau_\delta$.

The amplitude of the m-th harmonic of the current $i_0(t)$ is related to the dc component of the current i^0 like $2I_m(z)/I_0(z)$ ($I_m(z)$ is a modified Bessel function), and increases rapidly with increasing z, approaching 2. This corresponds to the turning of $i_0(t)$ into a δ-function shifted by π relative to the maximum of the total current $i(t)$ and by π/2 relative to the maximum of the field $E_0(t)$.

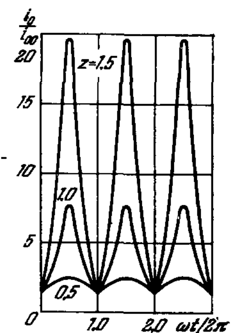

FIG. 14. Dependence of the avalanche current on the time and amplitude of a sinusoidal external signal.

By determining the ratio of the first voltage harmonic to the alternating current $\tilde{i}(t)$ from (4.4) and (4.12), we obtain approximate expressions for the total resistance of the p-n junction:

$$\omega CR = -\beta^2\Phi(z) \sum_{j=p,n} \frac{C}{C_j}\chi(\xi_j),$$
$$\omega CX = -\left[1 + \beta^2\Phi(z) \sum_{j=p,n} \frac{C}{C_j}\lambda(\xi_j)\right], \quad (4.13)$$

where

$$\Phi(z) = \frac{2}{z} f(z); \quad f(z) = \frac{I_1(z)}{I_0(z)}; \quad \lambda(\xi) = \frac{\sin\xi}{\xi} - \frac{\tau_\delta}{2\tau}.$$

These expressions differ from the simplified formulas of the linear theory (4.10), taken at $\sigma = 0$ and $\beta^2 \ll 1$, only in that β^2 is replaced by the factor $\beta^2\varphi(z)$, which is proportional to the ratio of the first harmonic of the conduction current $2f(z)i^0$ to the displacement current zi_x. At small oscillation amplitudes ($z \ll 1$), the first harmonic of the conduction current increases linearly with $z(f(z) \simeq z/2)$, but with increasing amplitude it reaches rapidly a maximum value ($f(z) \to 1$), so that the product $\beta^2\varphi(z)$, and consequently also the modulus of the negative resistance of the p-n junction $|R(z)|$ decrease in inverse proportion to z. The reactance of the p-n junction approaches $-1/\omega C$ in this case.

Similar results are obtained also in the case when the voltage $V(t)$, rather than the current in the external circuit, is sinusoidal. The formulas for R and X then coincide with (4.13), apart from terms of higher order with respect to β^2.

b) Multiplication nonlinearity. As indicated above, the function $\Psi(E_0)$ can be written approximately in the form $\Psi(E_0) \simeq (E_0/E_{br})^{n+l} \simeq (E_0/E_{pr})^6$. Using the space chage of the carriers (the condition $\beta^2 \ll 1$), and assuming the diode voltage to be a sinusoidal function of the time $V(t) = V_0 + V_1 \sin \omega t$, we arrive at the equation

$$\frac{\tau_\delta}{2}\frac{d\ln i_0}{dt} = \left(\frac{V_0}{V_{br}}\right)^6 (1 + \alpha\sin\omega t)^6 - 1, \quad (4.14)$$

where $\alpha = V_1/V_0$. Integration of (4.14) yields a formula that relates the dc bias on the diode to the amplitude of the alternating voltage $V_0/V_{br} = A(\alpha)$, and an expression for the current $i_0(t)$:

$$\ln\frac{i_0(t)}{i_{00}} = \frac{2}{\omega\tau_\delta}A(\alpha) + \sum_{k=1}^{6} B_k(\alpha)\cos k\omega t. \quad (4.15)$$

In the last expression, the higher coefficients $B_k(\alpha)$ amount to less than 0.3 of $B_1(\alpha)$ even at the maximum value $\alpha = 1$, so that in a qualitative analysis they can be neglected. The difference between (4.15) and (4.13) then reduces only to a replacement of z by $z' = \nu(\alpha)z$, so that expressions (4.12) for the impedance of the p-n junction remain in force. The function $\nu(\alpha)$ and also the change in the dc bias on the diode, are shown in Fig. 15. The minimum value of V_0 is equal to the maximum amplitude of the oscillations $V_{1\,max}$, corresponding to $\alpha = 1$, and

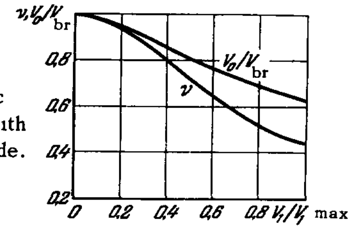

FIG. 15. Variation of the dc bias V_0 and the coefficient ν with the alternating-voltage amplitude.

amounts to $V_{0\,min} \simeq V_{1\,max} \simeq 0.64\ V_{br}$. The values of $\nu(\alpha)$ lie between 0.5 and 1.

Thus, the multiplication nonlinearity leads essentially only to a decrease of the dc component of the bias voltage with increasing oscillation amplitude; the influence of this nonlinearity on the amplitude dependence of the p-n junction impedance is negligible.

A more detailed analysis of Eqs. (3.1), (4.1), and (4.3), with allowance for the carrier space charge (β^2 not much smaller than 1) and for other factors neglected above, leads to the following expressions for the impedance of a symmetrical ($\tau_p = \tau_n = \tau$) p-n junction:

$$\omega CR = -\frac{C}{C'}\frac{y}{k}\Phi(y)\left[\chi(\xi)\cos\varphi - \lambda(\xi)\sin\varphi\right],$$
$$-\omega CX = 1 + \frac{C}{C'}\frac{y}{k}\Phi(y)\left[\lambda(\xi)\cos\varphi + \chi(\xi)\sin\varphi\right]. \quad (4.16)$$

Here y and φ are respectively the amplitude and phase of the first harmonic of the function $\ln(i_0/i^0) = y_0 - y\cos(\xi + \varphi)$, which are connected with the amplitude z' of the external sinusoidal signal by the relations

$$y^2\left[M^2(y) + N^2(y)\right] = z'^2; \quad \operatorname{tg}\varphi = \frac{N(y)}{M(y)};$$
$$N(y) = \beta\Phi(y)\left[a'I_0^2(y) + \gamma\eta\frac{\sin\gamma\xi}{\gamma\xi}\right];$$
$$M(y) = 1 - \beta^2\Phi(y)\cos\gamma\xi; \quad \gamma = \frac{\tau_\gamma}{\tau}; \quad k = \frac{i_{01}}{i^0}; \quad (4.17)$$
$$\eta = \Omega\tau; \quad a' = \frac{a}{\beta} - \frac{2}{\Omega\tau_\delta}\frac{i_s}{i^0}.$$

Unlike the simplified expressions (4.13), the formulas in (4.16) take into account the influence of the signal amplitude not only on the relative amplitude of the first current harmonic (the factor $\varphi(y)$), but also on the phase shift ($\pi - \varphi$) of this harmonic relative to the total current $i(t)$.

The ac component of the carrier space charge ($\beta^2 \neq 0$) and the saturation current ($a \neq 0$) cause this phase shift to increase with increasing oscillation amplitude from the small-signal value $\pi - \tan^{-1}[\sigma/(1-\beta^2)] \simeq \pi$ to $\pi - \tan^{-1}[\chi(\xi)/\lambda(\xi)]$. This increase reduces the modulus of the negative resistance to zero. The critical value of the oscillation amplitude, at which $R(z)$ reverses sign, decreases with increasing parameters $\beta^2 < 1$ and a, as shown in Fig. 16.

Thus the saturation current, which governs the value of the parameter a, is one of the main factors limiting the maximum oscillation amplitude, and is especially significant at small values of the transit

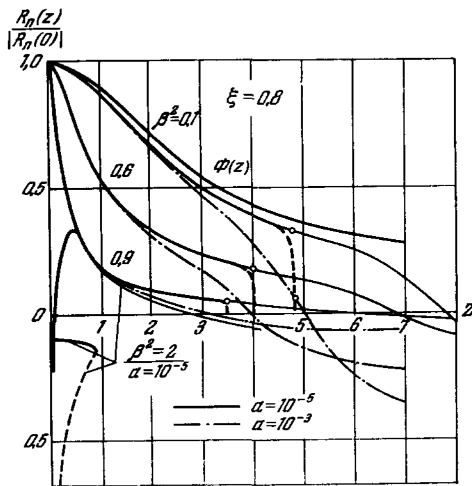

FIG. 16. Variation of the resistance of the ATD p-n junction with increasing amplitude of the high-frequency signal.

angle $\xi < 1$, when the principal role is played by the current nonlinearity. When $\xi \gtrsim 1$ and $i_s/i^0 \lesssim 10^{-3}$, this amplitude is limited by the condition* $V_{1\,max} \le V_{0\,min} \simeq 0.6\,V_{br}$ (the dashed cuves in Fig. 16). When $\beta^2 > 1$, as seen from Fig. 16, the function $R(z)$ may go over with increasing z from the region $R(z) > 1$ into the region $R(z) < 0$. Such a transition is connected with the decrease of the ratio of the conduction current to the displacement current with increasing z, and takes place when $\beta^2\varphi(z) \simeq 1$. This points to the possibility of hard excitation of oscillations in the ATD at the frequency ω and at currents exceeding the characteristic current for this frequency.

We have neglected above the nonlinear effect connected with the modulation of the p-n junction width by the alternating voltage. This modulation does not occur in a p-i-n ATD, in which the breakdown voltage greatly exceeds the voltage of through breakdown [14], but may play an important role in p-n ATD. In the latter, the modulation of the p-n junction width leads to an increase in its average capacitance, which can reach 16% for a gradual p-n junction, and can also cause additional parametric effects [3,16].

In addition, this modulation can, by varying the transit angle ξ, influence also the resistance of the p-n junction. This effect can be taken into account approximately by slightly underestimating the maximum value of the oscillation amplitude: $V_{1\,max} = 0.5\,V_{br} < 0.64\,V_{br}$.

5. OUTPUT POWER AND EFFICIENCY OF AN OSCILLATOR USING ATD

Using the results of the nonlinear analysis of the ATD, we can readily obtain relations for the main parameters of an ATD oscillator (ATDG), namely the frequency, power, and efficiency of self oscillations. For the microwave range, such an oscillator consists of an avalanche-transit diode and a cavity resonator coupled to the useful load. At a current value much lower than characteristic ($\beta^2 < 0.5$) and for a resonator with not too low a Q, the output of such an oscillator is nearly sinusoidal, and its analysis can be carried out by the well known method of slowly varying amplitudes [22]. In particular, the stationary values of the frequency and of the amplitude of the self oscillations are determined by the system of equations

$$X(\omega, z) + X_p(\omega) = 0, \tag{5.1}$$

$$R(\omega, z) + R_p(\omega) = 0, \tag{5.2}$$

where X_p and R_p are the reactance and resistance of the tank circuit of the oscillator, referred to the p-n junction. The tank circuit incorporates, besides the cavity and the load, also the crystal loss resistance R_s and the reactive parameters of the diode body.

Since the reactance of a p-n junction differs little from the reactance of its cold capacitance C when $\beta^2 \ll 1$, the frequency of the self oscillations ω_0 is determined approximately by the relation

$$X_p(\omega_0) \simeq (\omega_0 C)^{-1} \tag{5.3}$$

and depends relatively little on the working current and on the amplitude of the oscillations. Therefore to calculate the amplitude, and consequently also the output power of the oscillator, we can use Eqs. (4.16) and (5.2), in which we put $\omega = \omega_0$.

The total oscillation power P_e delivered by a symmetrical p-n junction to the external circuit and the electronic efficiency η_e of the oscillator, are functions of the oscillation amplitude $z = i_{01}/i_x$:

$$P_e = \eta_e i^0 V_0 = -\frac{(i^0)^2 R(z)\cdot z^2}{2\beta^4}. \tag{5.4}$$

This power reaches a maximum value P_{em} at a certain optimal value $z = z_m$.

At small transit angles, the values of z_m are determined by the saturation current, which limits the maximum amplitude of the alternating current of the diode (current limitation). When $\xi \ge 2$, the decisive factor is the limitation of the amplitude of the alternating voltage (the condition $V_1 < 0.5V_{br}$). To estimate the values of P_{em} and η_{em}, we neglect, for $z \le z_m$, the saturation current, putting in (4.16) $\sigma = 0$ and $\psi = \pi$; then $R(z) \simeq (\omega C)^{-1} f(y)\chi(\xi)$ and

$$P_e \simeq \frac{i^0 i_1}{\omega C}\cdot f(y)\cdot \chi(\xi). \tag{5.5}$$

At large oscillation amplitudes ($z, y \gg 1$) we can neglect also the ratio of the conduction current to the total current (putting $\beta^2\varphi(y) \ll 1$) and assume the avalanche current to be a δ-function of the time. Then we can put in (5.5) $i_1 \simeq \omega C V_1$ and $f(y) \simeq 1$, which yields

*When $V_1 > V_0$, current will flow through the diode in the forward direction.

$$\eta_e \simeq \frac{V_1}{V_0}\frac{C'}{C}\cdot\chi(\xi). \qquad (5.6)$$

The function $\chi(\xi)$ goes through a maximum $\chi = \chi_m \simeq 0.73$ when $\xi = \xi_m \simeq 2.3$. Therefore the maximum of η_{em}, corresponding to the limiting oscillating amplitude $V_{1m} = V_0$, amounts to

$$\eta_{em} \simeq 0.73\frac{C}{C'}. \qquad (5.7)$$

In practice, however, the condition $V_1 = V_0$ is difficult to realize owing to the modulation of the p-n junction width. By specifying a more likely value $V_{1m}/V_0 \simeq 0.7$, corresponding in a p-n ATD to $V_{1m} = 0.5V_{br}$, we get

$$\eta_{em} \simeq 0.5\frac{C}{C'} \simeq 0{,}5\left(1-\frac{\delta}{W}\right). \qquad (5.8)$$

According to (5.8), the maximum electronic efficiency of an ATD oscillator increases with decreasing relative width of the multiplication layer and can reach 50%. For an ATD with a stepwise and continuous p-n junction we have respectively $C/C' \simeq 4/5$, $\eta_{em} \simeq 40\%$ and $C/C' \simeq 2/3$, $\eta_{em} \simeq 33\%$.

Formula (5.6) can be readily obtained also directly by determining the energy of interaction between a high-frequency electric field and a δ-like electron packet leaving the multiplication layer at the instant of time when the high-frequency electric field in the transit section passes through zero, and changes from accelerating to decelerating.

The results of a more rigorous calculation of η_{em}, carried out by means of formulas (4.16) and (5.4) under the condition $V_1 = 0.7\,V_0$ with account taken of the actual form of $i_0(t)$ and the phase shifts due to the parameters a and β^2, are shown in Fig. 17a.

The function $\eta_e(\xi)$ has a gently sloping maximum near $\xi \simeq 2$, the magnitude of which depends little on a but decreases with increasing β^2 from 0.45 C/C′ when $\beta^2 = 0.1$ to 0.36 C/C′ when $\beta^2 = 0.6$ (cf. (5.8)).

The useful power P_L dissipated in the active load R_L is always smaller than P_e, owing to the losses in the cavity and in the diode. The maximum value of this power, $P_L = P_{Lm}$, corresponding to the optimal

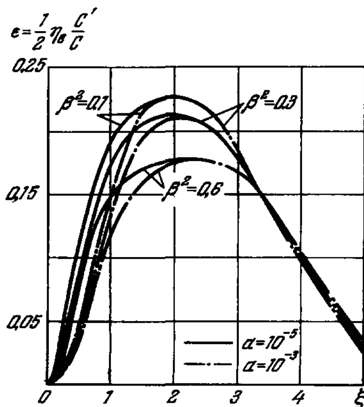

FIG. 17a. Maximum electronic efficiency of ATD oscillator.

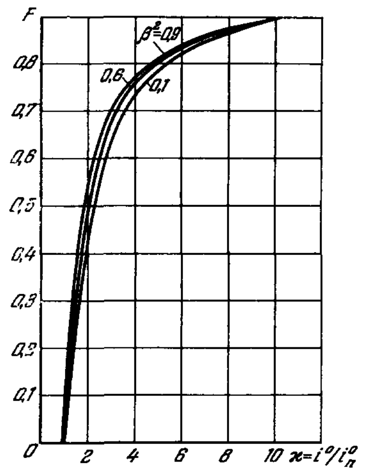

FIG. 17b. The function $F(\kappa)$.

load $R_L = R_{Lm}$ in the absence of cavity losses and for $V_1 < 0.5\,V_{br}$, is determined by the approximate expression

$$P_{Lm} = \frac{(i^0)^2}{2\omega C}\left[\frac{C}{C'}\chi(\xi)\right]^2 Q_s\cdot F(\varkappa), \qquad (5.9)$$

where $Q_s = (\omega C R_s)^{-1}$ is the Q of the diode, $\kappa = i^0/i_{st}$ is the ratio of the working current i^0 to the starting current of the generator at minimum load i_{st}, and $F(\kappa)$ is a function plotted in Fig. 17b. When $\kappa \geq 3$ and $\xi = 2.3$ we have $F(\kappa) \simeq 1$, $\chi^2 \simeq \chi_m^2 \simeq 0.52$, and

$$P_{Lm}(2{,}3) = P_{Lmm} \simeq 0{,}25\frac{(i^0)^2}{\omega C}\left(\frac{C}{C'}\right)^2 Q_s. \qquad (5.10)$$

According to (5.9) and (5.10) the total efficiency of the oscillator, $\eta_{Lm} = P_{Lm}/i^0V_0$, is proportional to the current, to the Q of the diode, and to the reciprocal of its capacitance; it reaches a maximum value at $\xi \simeq 2.3$.

6. CURRENT FLUCTUATIONS AND NOISE PROPERTIES OF ATD AND ATDO

A characteristic feature of avalanche-transit diodes is the increased noise level at high frequencies ($> 10^4$ Hz). Even in germanium diffusion ATD with homogeneous breakdown this level is 25—30 dB higher than the shot noise of a vacuum diode with the same current. In silicon ATD, where the breakdown is accompanied by microplasma phenomena, this excess can reach 60—70 dB [16]. Detailed investigations have shown that, at least in germanium ATD, the excess noise is due not to extraneous effects, but is a direct consequence of the statistical peculiarities of the avalanche process of impact ionization [3,23,24].

The common origin of all the particles of an avalanche produced by passage of an electron or hole through the multiplication layer, and the correlation between the succeeding ionization processes, cause the probability distribution P(M) of the number M of particles in the avalanche to differ from a Poisson distribution, and if the electron and hole ionization

coefficients are equal the probability distribution is given by

$$P(M) = D_M \Psi^{M-1} e^{-M\Psi}, \quad (6.1)$$

where $\Psi = \int_{-W_n}^{W_p} \bar{\alpha}\, dx$ is the integral multiplication and D_M are numerical coefficients. The mean square and the variance of the number of particles in the avalanche are connected with the mean value (multiplication coefficient) $\overline{M}$ by the relations

$$\overline{M^2} = (\overline{M})^3, \quad \Delta\overline{M^2} = \overline{M^2} - (\overline{M})^2 = (\overline{M})^2(\overline{M} - 1), \quad (6.2)$$

i.e., they greatly exceed the corresponding values for independent events, which, as is well known, are $\overline{M}^2 = (\overline{M})^2 + \overline{M}$ and $\overline{\Delta M^2} = \overline{M}$.

The fluctuations of the avalanche current i_0 are made up of fluctuations of the primary carrier current - the saturation current i_s—and the fluctuations of the multiplication coefficient M. Inasmuch as the avalanche does not develop instantaneously but within a time of the order of $\tau_\delta \ln M$, the latter depends not only on $\overline{\Delta M^2}$, but also on the frequency and on the damping action of the space charge of the carriers in the transit sections. A calculation in which allowance is made for the foregoing factors gives the following approximate expression for the spectral density of the fluctuations of the avalanche current $S_0^i(\omega)$ in a p-n junction that is short circuited at high frequency:

$$S_0^i(\omega) - S_s(\omega)\overline{M^2} B(\omega, \beta^2, \xi), \quad (6.3)$$

where

$$B(\omega, \beta^2, \xi) = \left\{ \left(\frac{\omega}{\omega_M}\right)^2 [1 - \beta^2 \cdot \mu(\xi)]^2 + \left[1 + \beta^2 \cdot \chi(\xi) \frac{\omega}{\omega_M}\right]\right\}^{-1},$$

$S_s(\omega)$ is the spectral density of the saturation current fluctuation, and $(\omega_M)^{-1} = M\tau_\delta/2$ is the characteristic time, which is connected with the avalanche development time. At the values typical of germanium ATD, $M \simeq 10^2 - 10^4$, $\delta \simeq 10^{-4} - 10^{-5}$ cm, and $v \simeq 6 \times 10^6$ cm/sec, we have

$$\frac{\omega_M}{2\pi} \simeq 10^6 \div 10^8 \text{ Hz}$$

Assuming the fluctuations of the current i_s to be of the shot type and taking (6.2) into account, we get

$$S_0^i(\omega) \simeq 2ei^0 (\overline{M})^2 B\left(\frac{\omega}{\omega_M}, \beta^2, \xi\right). \quad (6.4)$$

At frequencies below ω_M we have $B(\omega, \beta^2, \xi) \simeq 1$, and S_0^i exceeds by a factor $(\overline{M})^2$ the density of the shot fluctuations, is not damped by the space charge, and depends strongly on the temperature (like i_s^{-2}) for a specified value of the diode current i^0.

At frequencies larger than ω_M we have approximately

$$B(\omega, \beta^2, \xi) \simeq \left(\frac{\omega_M}{\omega}\right)^2 [1 - \beta^2\mu^2(\xi) + \beta^4 \cdot \chi^2(\xi)]^{-1}. \quad (6.5)$$

In this case the function $S_0^i(i^0)$ goes through a maximum equal to

$$S_{0m} \simeq 2ei^0 \frac{\tau}{\tau_\delta} \chi^{-1}(\xi) \quad (6.6)$$

at a current determined by the condition

$$\beta_m^2 \simeq (\mu^2 + \chi^2)^{-\frac{1}{2}} \simeq \begin{cases} \frac{2}{\xi} & \text{if } \xi \lesssim \pi, \\ 1 & \text{if } \xi \gtrsim \pi. \end{cases}$$

According to (6.6), the quantity $S_0^i > 2ei^0$ does not depend on the saturation current (and consequently on the temperature), and when $\xi \lesssim \pi$ it changes in inverse proportion to the frequency.

At low frequencies ($< 10^4$ Hz), generation-recombination and flicker noise is superimposed on the shot noise. These types of noise have essentially the same character in ATD as in diodes of other types (see, for example,[25]).

If the diode is shunted by an impedance $Z_p(\omega) \neq 0$, the current fluctuations are accompanied by voltage fluctuations $S^V(\omega)$ on the p-n junction. Since the ATD is usually fed from a dc source to prevent thermal breakdown, we get at low frequencies $Z_p(0) \gg Z(0)$. The current fluctuations are then suppressed and the voltage fluctuations reach their maximum value

$$S^V(0) \simeq S^i(0) \cdot Z^2(0) \simeq S^i(0) \cdot R_0^2, \quad (6.7)$$

where R_0 is the differential resistance of the p-n junction. The fluctuations $S^i(\omega)$ and $S^V(\omega)$ are the main causes of noise in ATD oscillators and amplifiers.

The theoretical value of the noise figure of an ATD amplifier for the centimeter band is approximately 25—30 dB. The calculated value of the ratio of the signal power to the power of the amplitude noise in an ATD oscillator at frequencies within the pass band of the oscillator tank circuit is 145—155 dB/Hz.

7. RESULTS OF AN EXPERIMENTAL INVESTIGATION OF ATD CHARACTERISTICS

Experimental investigations of the electric characteristics and a check on the deduction of the ATD theory were carried out with diffusion germanium p-n ATD with symmetrical p-n junction and breakdown voltages 10—40 V by V. L. Aronov and A. I. Mel'nikov in 1960—1962. In particular, they measured the impedance of the ATD under working conditions in a wide range of frequencies, from the lowest ones to microwaves.

At low frequencies (< 1 MHz) it was observed that the impedance of the diode, which is equal to its differential resistance R_d, is two or three times larger than the value of R_0 given by (3.7), and decreases with increasing frequency. It turned out that this effect is connected with heating of the p-n junction by the flowing current, accompanied by an increase in the break-

down voltage V_{br}. At high frequencies, when the period of variation of the current is much shorter than the thermal relaxation time, the temperature of the p-n junction has no time to change within the period of the oscillation and its differential resistance coincides with R_0. On the other hand, if the period of the oscillations is large compared with the time of thermal relaxation, then the temperature T of the p-n junction is determined by the instantaneous value of the diode current i(t). The differential resistance, measured in the static mode or at very low frequencies ($\ll$ 1 MHz) is equal not to $R_0 + R_s$, but to

$$R_{st} = R_0 + \frac{dV_{br}}{di} + R_s. \tag{7.1}$$

Recognizing that $V_{br}(T) = V_{br}(T_0)[1 + d(T - T_0)]$, with $d \simeq 10^{-3}$ deg^{-1} for germanium diodes, and putting $T - T_0 = R_T i^0 V_{br}$, we get

$$R_{st} = R_0 + R_s + d^2 V_{br}^2 R_T. \tag{7.2}$$

By measuring R_{stat}, R_0, and the $R_d(\omega)$ dependence, we can obtain an important parameter of the ATD – its thermal resistance R_T, and also the time of thermal relaxation, which determines the maximum permissible value of the diode current in the continuous and pulsed modes.

The values of the product $(R_0C)_{exp}$, obtained from measurements at frequencies on the order of 1 MHz, are close to the calculated value $\tau/2$, but are always somewhat larger: For good diodes, as a rule, $(R_0C)_{exp} \simeq (1.2 - 1.5)\,\tau/2$. This discrepancy is apparently due to the fact that the breakdown encompasses only part of the area of the p-n junction: $S_1 < S$, with $S_1/S \simeq (\tau/2)(R_0C)^{-1}_{exp}$.

At current densities exceeding 10^4 A/cm^2, for ATD with $V_{br} \simeq 30$ V, one observes as a rule a monotonic increase of R_0 with increasing current, in accord with the theory (see (3.3)).

Typical plots of the small-signal impedance of the ATD p-n junction against the diode current and against the frequency, in the microwave band, are shown in Fig. 18. Comparison of Fig. 18 with Fig. 10 shows a good qualitative agreement between the experimental and theoretical curves. From the quantitative point of view this agreement is characterized by Fig. 19, which shows the calculated and the experimental values of the characteristic current as a function of the square of the frequency. Within the limits of the measurement errors, which are indicated by the vertical bars, the experimental dependence agrees with the calculated one $i_x(\omega) \sim \omega^2$. However, the absolute values of the characteristic current are larger than the theoretical ones. This discrepancy exceeds

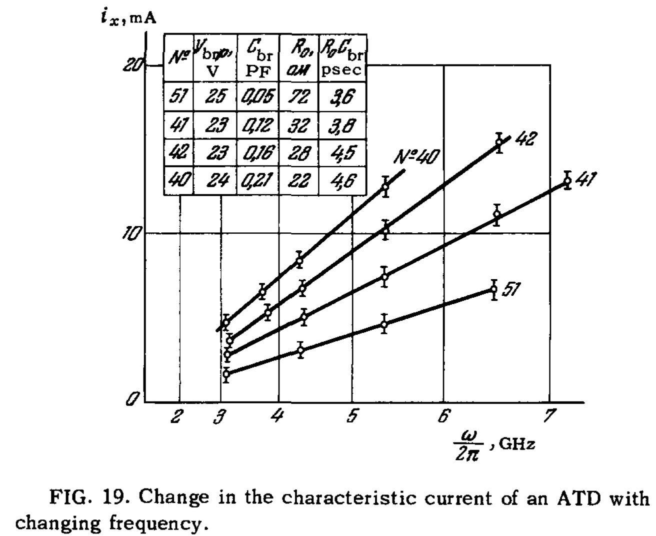

№	V_{br}, V	C_{br}, PF	R_0, ом	R_0C_{br}, psec
51	25	0,05	72	3,6
41	23	0,12	32	3,8
42	23	0,16	28	4,5
40	24	0,21	22	4,6

FIG. 19. Change in the characteristic current of an ATD with changing frequency.

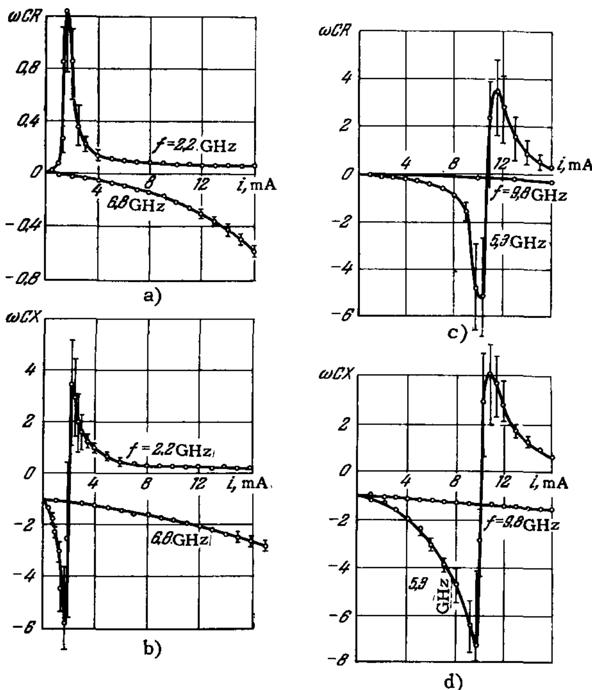

FIG. 18. Experimental plots of the resistance and reactance of the p-n junction of an ATD vs. the diode current.

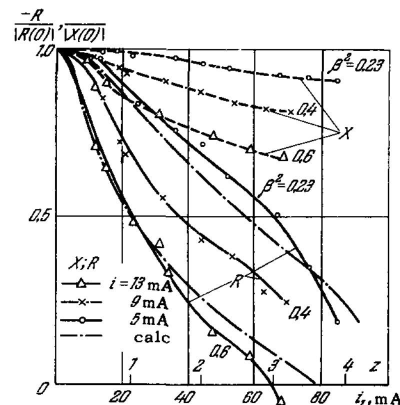

FIG. 20. Experimental plot of the impedance of the ATD p-n junction vs. the amplitude of the high-frequency signal. Comparison with calculation.

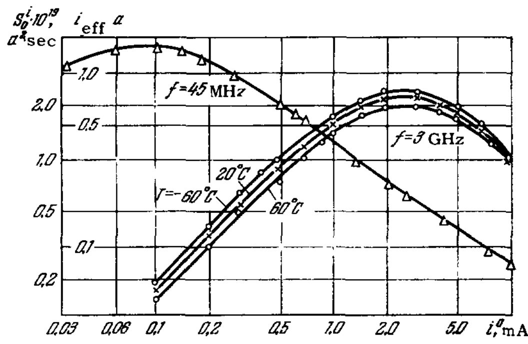

FIG. 21. Spectral density of ATD current fluctuations ($i_{eff} = s_0^i/2e$).

the measurement error, and its reason is unclear.

Plots of the resistance and reactance of the ATD vs. i_1 of the microwave signal are shown in Fig. 20. Here, too, satisfactory agreement is observed between the experimental data and the theoretical ones.

Experimental investigations of the current fluctuations and noise of ATD at high frequencies have confirmed the main deductions of the theory. Typical curves describing the variation of the spectral density of the ATD current fluctuations with frequency, diode current, and ambient temperature are shown in Fig. 21. In accordance with the theory, the function $S_0^i(i^0)$ goes through a maximum $S_m(\omega)$ at a diode current i_m^0, which increases with frequency. The value of $S_m(\omega)$ exceeds by 2—4 orders of magnitude the usual level of shot fluctuations $2ei^0$, decreasing with increasing frequency.

The spectral density of the fluctuations at high frequencies $\omega/2\pi > 10$ MHz is practically independent of the saturation current and of the multiplication coefficient. This is evidenced, first, by the small difference between the values of $S^i(\omega)$ for different diodes whose saturation currents differ by 1—2 orders of magnitude, and second, by the weak dependence of $S^i(\omega)$ on the ambient temperature: the relative change of $S^i(\omega)$ with change in temperature does not exceed 0.02 dB/deg at these frequencies.

Perfectly satisfactory results are obtained also by comparing the experimental and theoretical values of the main parameters of ATD generators. An illustration is Fig. 22, which shows the theoretical and experimental values of the output power of a single-loop generator, for a large number of ATD, as obtained by I. M. Martirosov. In the calculation use was made of formula (5.9), in which the experimental value of the ratio of the working current to the starting current was substituted. All these data lead to the conclusion that the initial ideas concerning the operating mechanism of the p-n ATD, and the theoretical deductions based on these ideas are all correct.

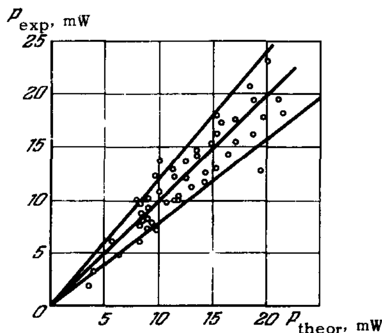

FIG. 22. Comparison of experimental and theoretical values of the power of an ATD generator.

Recently, reports were published of experimental investigations in the USA of the Read diode and of ATD on the basis of Si and GaAs [15,16,26]. The Read diode was designed for 180 MHz. The measured values turned out to be in satisfactory agreement with the calculation [15]. In [26], the linear parameters of the equivalent circuit of the p-n junctions of several epitaxial silicon p-n ATD were calculated with allowance for the real structure of these diodes. The experimental data are in qualitative agreement with the calculated ones, the quantitative discrepancy in them not exceeding 50%.

8. ACTIVE DEVICES WITH ATD

Besides theoretical and experimental investigations of the operating mechanism of the ATD, comprehensive technological and design work was done in the USSR in 1962—1964 on the construction of avalanche-transit diodes and active microwave devices based on them, intended for their use in miniaturized and economical microwave apparatus [3,4]*.

The best results were obtained with germanium diodes. As a result of improvements in the diffusion technology [27], ATD were developed with breakdown voltages V_{br} from 10 to 60 V, with capacitance $C_{V_{br}} \simeq 0.05 - 0.5$ pF, a time constant $R_sC \simeq 0.5 \simeq$ psec, and a thermal resistance 50—100 deg/W. These diodes were used to construct generators of coherent oscillations (ATDG) of different types, quartz-controlled multiplication networks, regenerative amplifiers for the centimeter and millimeter bands, and miniaturized microwave noise sources.

Generators of Coherent Oscillations for the Centimeter and Millimeter Wave Bands

Miniature generators for the centimeter bands (3—15 GHz) deliver in the continuous mode an output power from 5 to 50 mW at 3—7% efficiency when fed with a current of 10—20 mA and a voltage 20—70 V.

*The technology of ATD production was developed by a group headed by A. V. Krasilov and V. M. Val'd-Perlov, while active devices with ATD were developed under the direction of the author by engineers A. I. Mel'nikov, A. V. Skidan, A. D. Khodnevich, A. M. Tsebiev, and others.

FIG. 23. ATDG with a large range of mechanical frequency tuning.

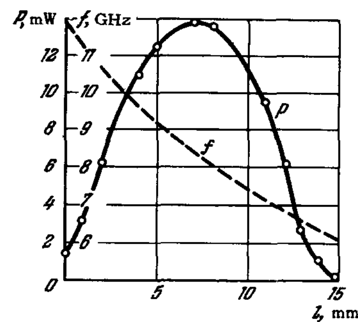

FIG. 24. Variation of the output power and of the frequency of ATDG when the coaxial plunger is displaced.

The oscillation frequency is determined by the reactive parameters of the diode and of the external circuit. An ATD with this value of V_{br} can operate efficiently in a frequency interval on the order of one octave. With increasing V_{br}, this interval shifts (owing to the increase in the transit angle) towards longer wavelengths. The indicated interval can be covered by a single generator with a coaxial-type tank circuit (Fig. 23) [28]. An example of the band width characteristic of such a generator is shown in Fig. 24.

Generators with a small tuning range can be constructed in miniature form using the intrinsic tank circuit of the ATD, made up of the p-n junction capacitance and the inductance of the diode body [29]. Photographs of such generators with coaxial and waveguide output lines are shown in Fig. 25.

The maximum oscillation power is limited by the allowable temperature of the p-n junction and by the maximum dissipated power. Using a quasicontinuous supply mode or cooling the diode to a temperature −50 to −100°C it is possible to increase the output power by a factor of 2 or more. An appreciable increase in the ATDG power can be obtained also by connecting several diodes in one resonant circuit. By arranging, for example, the diodes symmetrically on a circle near the side wall of a cylindrical resonator, it is possible to ensure effective addition of power from 4, 6, and more diodes with a suitable increase in the output power of the generator to 100 mW and more in the continuous mode [30].

Electric tuning of ATD generators is effected either by varying the diode current (in a narrow range), or with the aid of an additional varactor diode. In the latter case, the interval of electric frequency tuning of a generator in the centimeter band can reach 3—5%. One variant of a generator of this type is shown in Fig. 26; its pass band characteristic is shown in Fig. 27.

The large contents of harmonics in the spectrum of the avalanche current makes it possible to use cm-band ATD to produce mm-band generators [3]. The resonator of such a generator is best made of the two-loop or three-loop type in order that one of the loops, which is not coupled to the useful load, be tuned to the fundamental frequency in the short-wave part of the centimeter band (10—15 GHz), and the others to higher harmonics of this frequency. Lowering of the breakdown voltage to 10—12 V makes it possible to construct generators with a fundamental frequency lying in the millimeter band. Generators of this type have in the upper part of the millimeter band an output power on the order of several milliwatts (in the continuous-wave mode). The oscillation spectrum of a reflex klystron, although at frequencies sufficiently far from the center of the spectral line (by 0.1 MHz and more), where the main noise source are shot fluctuations of the avalanche current, the spectral density of the amplitude and frequency fluctuations of the ATDG are 15—20 dB higher than in the better reflex klystrons.

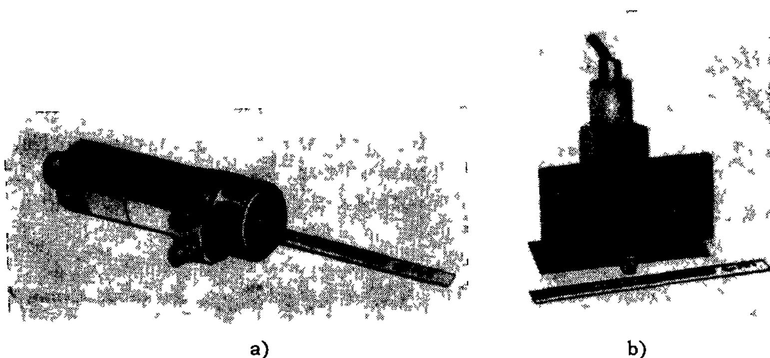

a) b)

FIG. 25. Miniaturized ATDG, a) coaxial, b) waveguide.

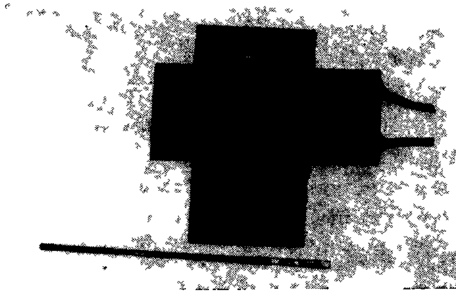

FIG. 26. ATDG with electric frequency tuning

Synchronization of ATDG by an External Signal and Quartz Controlled Multiplication Networks

The low negative Q of ATD and the fact that self-oscillating systems with these diodes are not isochronous makes possible effective synchronization of the generators by means of an external signal at either the fundamental frequency of the self oscillations or at its harmonics or subharmonics [3].

Synchronization of ATDG at the fundamental frequency is attained at synchronizing-signal powers P_s which are lower by 40—60 dB than the power of the free self oscillations (Fig. 28a). In the case of synchronization at the harmonics of the self oscillations, at low harmonic numbers $n = \omega_s/\omega_0 \simeq 3$—4, the power of the synchronizing signal can also be lower than the power of the self oscillations of the ATDG by 10—15 dB (Fig. 28b). This makes it possible to use ATDG for frequency division in the millimeter band.

ATDG can be synchronized by a low-frequency signal (at the subharmonics of the self oscillations) either by applying a low-frequency signal directly to the ATD, or by using an additional multiplication stage with a varactor or some other multiplying diode. In either case, for effective synchronization of ATDG in the centimeter band, by means of a signal in the meter band (at subharmonics 30—60) the required power of the latter does not exceed 200—300 MW. This principle can be used to construct miniature quartz-controlled multiplication networks with output stage consisting of an ATDG in the centimeter band

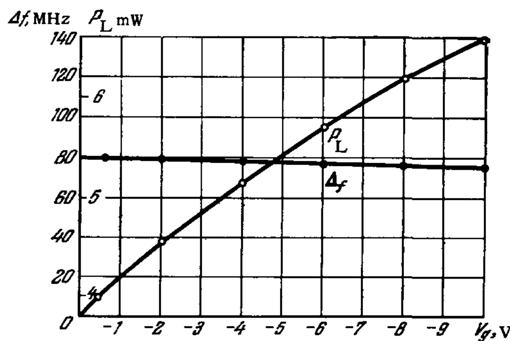

FIG 27 Variation of ATDG output power and frequency vs varactor voltage

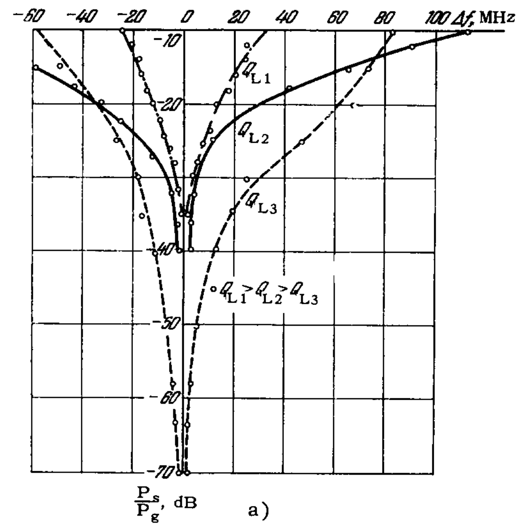

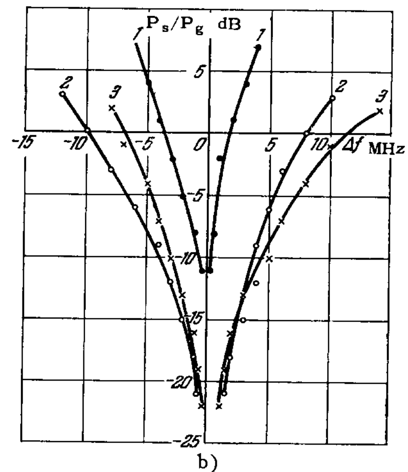

FIG 28 Limits of ATDG synchronization band vs ratio of the synchronizing-signal power P_s to the free self-oscillation power P_g at different values of the loaded Q of the generator Q_L (curves 1, 2, 3) a) Fundamental frequency ($\omega_s = \omega_0$), b) third harmonic ($\omega_s = 3\omega_0$)

and with long-time relative frequency stability 10^{-7}—10^{-8} and a low level of phase fluctuations. Such stable microwave-signal sources are superior to the presently known multiplication networks with varactors in that the number of intermediate stages is much smaller, the cost is lower, and the reliability is higher. The simplicity and efficiency of external synchronization of ATD generators and their small dimensions make it possible to use these devices to construct multi-element active transmitting and receiving antenna arrays. In the transmitting arrays, the use of a large number of coherent ATDG radiators synchronized by an external signal makes it possible to shape the radiation beam and to effect electric scanning of this beam in space by varying the phase differences of the oscillations of the different generators. In receiving arrays, the synchronized ATDG can be used as coherent heterodynes.

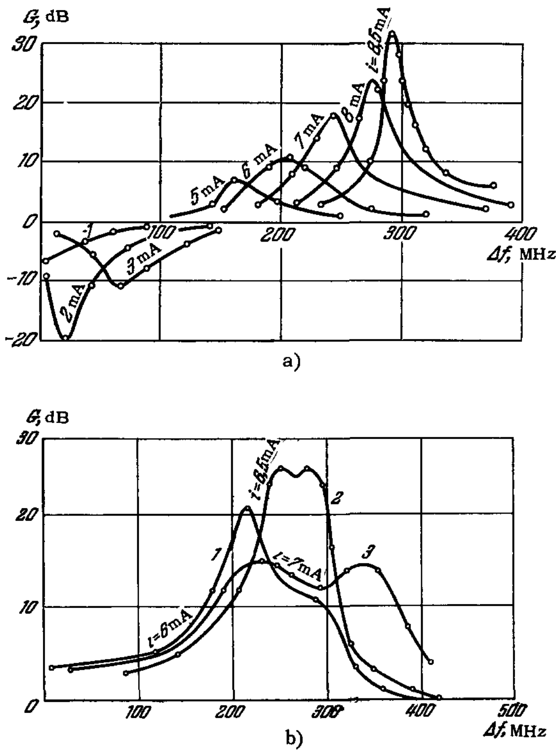

FIG. 29. Frequency dependence of the gain G of an ATD amplifier. a) For single-loop amplifier, b) for two-loop amplifier.

ATD Regenerative Amplifiers

ATD can be used not only for generators but also for generative amplifiers. At 25—30 V and 2—5 mA, a single-loop 3-cm amplifier provides in the continuous mode a stable gain G = 20—30 dB in a bandwidth up to 50 MHz (Fig. 29a). The use of two-loop resonant systems makes it possible to broaden the band of the amplifier to 100—150 MHz (Fig. 29b). The amplitude characteristic of the amplifier remains linear at an input-signal power P_{in} lower than 10^{-6} W (Fig. 30). A feature of a regenerative ATD amplifier is small size and simple construction, but its application is limited by the large value of the noise figure, of the order of 25—30 dB, due to the

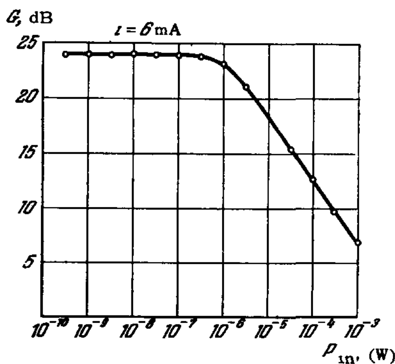

FIG. 30. Amplitude characteristic of ATD amplifier.

high level of shot fluctuations of the avalanche current.

Besides the ordinary regenerative negative-resistance amplifier, the specific features of the ATD make it possible to effect amplification which can be called autoparametric. The self oscillations in ATD generators are accompanied by modulation of the p-n junction capacitance, which can, if the microwave tank circuit is suitably tuned, give rise to parametric regeneration at frequencies different from the self-oscillation frequency. An autoparametric amplifier constructed on this principle provided a gain exceeding 20 dB at an operating frequency of GHz and at a self-oscillation frequency of approximately 10 GHz[31].

Noise Generators[4]

According to formula (6.6), at frequencies $\omega > \omega_M$ the high spectral density of the avalanche-current fluctuations does not depend on the saturation current (multiplication coefficient M) and is determined only by the value of the frequency and of the current of the diode. This points to the possibility of using semiconductor diodes of the ATD type, in which the avalanche breakdown develops uniformly over the area of the p-n junction, as sources of stable white noise of high intensity.

The noise generators of this type developed for measuring purposes (ATDNG) cover the decimeter and centimeter bands. A photograph of one version of ATDNG for the decimeter band is shown in Fig. 31. At a supply power 10—100 MW (voltage 10—15 V, current 0.5—10 mA) the effective noise temperature of these generators lies in the range from 10^5—10^{6}°K in the short-wave part of the centimeter band to 10^7—10^8°K in the decimeter band, and can be smoothly regulated by varying the diode current. The generators are characterized by temperature and long-time stability of noise level which is sufficiently high for measuring purposes, and permit modulation by microsecond pulses. This property of the ATDNG and also their small dimensions, low supply power, and high noise level determine the significant advantages of these devices over the hitherto known measuring noise generators using gas-discharge tubes and vacuum diodes.

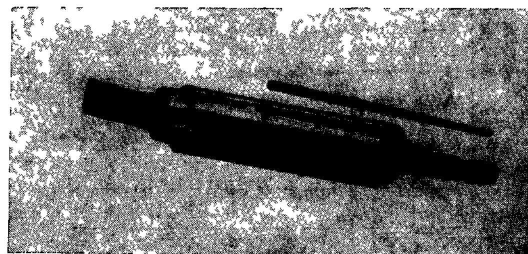

FIG. 31 ATD noise generator.

From the foregoing brief description of certain domestic microwave ATD devices we see that even now this new device is not only of physical but also of considerable practical interest. Microwave generators with ATD offer serious advantages with respect to size, weight, economy of power supply, and cost both over corresponding vacuum devices - reflex klystrons - and over multiplying networks with varactors. At the present time they are used successfully to produce miniaturized and economical microwave apparatus for various purposes, consisting entirely of solid-state elements. An example of such apparatus is the portable communication radio station for the centimeter band, developed in the USRS under the direction of S. A. Peregonov, in which the main microwave device performing the function of both the transmitting generator and the heterodyne, is an ATDG similar to that shown in Fig. 26.

Abroad, judging from the data published up to the beginning 1966 [5,6,16,20,32–38], ATD and microwave devices based on these diodes are being developed in the USA and Japan.* Although in 1965 none of these investigations went beyond the stage of initial laboratory research, they yielded many new interesting results. The ATD used in the USA are diodes based on silicon and gallium arsenide with a single diffusion p-n junction, produced either in a uniformly doped material or in a high-resistance epitaxial film. The insufficient heat dissipation and the inhomogeneity of the p-n junction make it difficult to operate the diode in the continuous mode, so that most research has been carried out in the pulsed mode. Generation was attained in the 0.9—4 GHz with silicon planar diodes with breakdown voltage 120 V, mounted in a coaxial resonator, at a cw output power near 1 MW with efficiency 0.5%. In the pulsed mode the same diodes used in a waveguide tank circuit generated oscillations in the 10—15 GHz band with output powers up to 100 MW [32]. Silicon diffusion mesa diodes with breakdown voltage 7—55 V in waveguide tank circuits of appropriate cross section generated (in the pulsed mode) oscillations in the range from 10 to 15 GHz at a current from 0.15 to 1.5 A. The generation frequency increased approximately in inverse proportion to the breakdown voltage. The output power reached 350 MW at 50 GHz and 1—2 MW at 85 GHz [33].

The maximum output power obtained with silicon diodes in the continuous mode is approximately 13 MW at 10.5 GHz and 0.5% efficiency for a simple diffusion diode, and approximately 19 MW at 5 GHz and 1.4% efficiency for an epitaxial diffusion diode with p^+-n-i-n^+ structure close to that proposed by Read [14,16].

Parametric epitaxial gallium-arsenide diodes with breakdown voltage 20—70 V in the avalanche multiplication mode generated oscillations in the 8—30 GHz band. In the pulsed mode, at a current density 10^3—10^4 A/cm^2, an output power of 40 MW was obtained at 27 GHz and 2% efficiency, while in the continuous mode the maximum output power reached 22.5 MW at 13 GHz and 4.25% efficiency [6,34,35].

Although the main mechanism of the observed generation has apparently an avalanche-transit character and is not connected directly with the main instability in the volume (the Gunn effect [39]), the latter can take place in the barrier layer of the p-n junction, where the electric field intensity is sufficiently high. It is therefore not excluded that the combination of avalanche and domain instability can increase the efficiency of GaAs ATD [35]

No detailed investigations of the oscillation spectrum are reported in the cited papers, and the fundamental-frequency line width measured with a spectrum analyzer is close to the value 10—50 kHz which is customary for microwave self oscillators. In many cases parametric excitation of low-frequency oscillations and generation of higher harmonics were observed [16,34]. These effects apparently explain the wide range of generation frequencies observed by different workers.

At currents below the generation threshold, many authors observed regenerative amplification of oscillations fed to the input of a resonator with ATD through a circulator. A gain of 20 dB was obtained with silicon diodes at a frequency 11 GHz and a band width of 20 MHz, and a noise figure 50—60 dB [16,36].

In Japan, microwave generation was obtained with a germanium diffusion diode in the pulsed mode. The oscillations were observed in a wide range of frequencies, up to 90 GHz [37]*.

Comparing the results obtained with avalanche-transit diodes of germanium, silicon, and gallium arsenide, we can note the following. The main advantage of germanium ATD is the homogeneity of the p-n junction, which ensures uniform development of the breakdown over its area, and the high thermal conductivity of the germanium, which makes it possible to lower the thermal resistance of the diode. A shortcoming of these diodes is the small width of the forbidden band in Ge (0.7 eV) and the associated low values of the limiting temperature of the p-n junction (100—120° C) and the increased saturation current.

In silicon and gallium arsenide, the width of the forbidden band is approximately double that in germanium (1.21 eV in Si and 1.32 eV in GaAs), and the carrier drift velocities are also higher. However, the ensuing advantages of Si and GaAs have not yet been realized in ATD, owing to the inhomogeneity of the

*Research work in this direction was started also in West Germany [40,41].

*p-i-n diodes with breakdown voltage exceeding 100 V were investigated in West Germany. Simultaneous generation at several frequencies from 1.5 to 6 GHz was observed with a total pulse power of approximately 4 3 W [40].

breakdown of the p-n junctions in these materials. Lattice defects and microscopic inclusions, which cause local breakdown (microplasma), greatly reduce the permissible level of power dissipation, deteriorating the reliability and other characteristics of the devices. As a result, the main parameters of the germanium ATD turned out to be better at the present time.

Further progress in ATD technology will be apparently very closely related with progress in the technology of manufacturing homogeneous p-n junctions in Si, GaAs, Ge, and other semiconductor materials.

[1] A. S. Tager, A. I. Mel'nikov, G. P. Kobel'kov, and A. M. Tsebiev, Author's Certificate (Patent Disclosure) No. 185965, Priority 27 October 1959.

[2] A. S. Tager, A. I. Mel'nikov, G. P. Kobel'kov, and A. I. Tsebiev, Diploma for Discovery No. 24, Priority 27 October 1959.

[3] A. S. Tager. Generation and Amplification of Microwave Oscillations with the aid of Diodes with Dynamic Negative Resistance. Doctoral dissertation, Moscow, 1962.

[4] V. M. Val'd-Perlov, A. V. Karsilov, and A. S. Tager, Radiotekhnika i élektronika 11, No. 11, 2008 (1966).

[5] R. L. Jonston, B. C. De Loach, B. G. Cohen, Bell Syst. Techn. J. Briefs 44, 369 (1965).

[6] F. A. Brand, V. I. Higgins, I. I. Baranowski, M. A. Druesne, Proc. IEEE 53, 1276 (1965).

[7] W. E. Benham, Phil. Mag. 5, 641 (1931), 11, 457 (1933).

[8] I. Müller, Hochfrequenz und Elektroakustik 41, 156 (1933).

[9] G. A. Grinberg, JETP 6, 126 (1936).

[10] F. B. Llewellyn, A. E. Bowen, Bell Syst. Techn. J. 18, 280 (1939).

[11] F. B. Llewellyn, Generation of Electrons (Russ. transl.), Gostekhizdat, 1946.

[12] O. Losev, Telegrafiya i telefoniya bez provodov (Wireless Telegraphy and Telephony) 14, 374 and 15, 564 (1922).

[13] W. Schockley, Bell Syst. Techn. J. 33, 799 (1954).

[14] W. T. Read, Bell Syst. Techn. J. 37, 401 (1958).

[15] C. A. Lee, R. L. Batdorf, W. Wiegmann, G. Kaminsky, Appl. Phys. Letts, 6, 89 (1965).

[16] B. C. De Loach, R. L. Jonston, IEEE Trans. ED-13, 181 (1966).

[17] J. Gunn, J. of Electronics 2, 87 (1956).

[18] A. C. Prior, J. Phys. Chem. Sol. 12, 175 (1960).

[19] G. E. Pikus, Osnovy teorii poluprovodnikovykh priborov (Fundamentals of the Theory of Semiconductor Devices), Nauka, 1965.

[20] T. Misawa, IEEE Trans. ED-13, 137, 143 (1966).

[21] A. P. Shotov, ZhTF 26, 1634 (1956) and 28, 437 (1958), Soviet Phys. Tech. Phys. 1, 1591 (1957) and 3, 413 (1958).

[22] A. A. Andronov, A. A. Vitt, and S. E. Khaĭkin, Teoriya kolebaniĭ (Theory of Oscillations), Fizmatgiz, 1959.

[23] A. S. Tager, FTT 6, 2418 (1964), Soviet Phys. Solid State 6, 1919 (1964).

[24] R. I. McIntyre, IEEE Trans. ED-13, 164 (1966).

[25] A. Van der Ziel, Fluctuation Phenomena in Semiconductors, Butterworths, 1959.

[26] T. G. Josenhaus, T. Misawa, IEEE Trans. ED-13, 206 (1966).

[27] V. M. Val'd-Perlov, V. V. Veitz, and V. V. Voltsit, Author's Certificate No. 882974, Priority 6 August 1964.

[28] A. S. Tager and A. D. Khodnevich, Author's Certificate No. 955164, Priority 10 December 1963.

[29] A. S. Tager and A. D. Khodnevich, Author's Certificate No. 712102, Priority 25 July 1961.

[30] A. S. Tager and A. D. Khodnevich, Author's Certificate No. 963808, Priority 25 March 1965.

[31] D. I. Govorova, S. A. Peregonov, and A. S. Tager, Authors Certificate No. 950520, Priority 3 April 1963.

[32] M. I. Grace, H. T. Minden, Proc. IEEE 53, 1646 (1965).

[33] C. A. Burrus, Proc. IEEE 53, 1256 (1965).

[34] V. I. Higgins, F. A. Brand, I. I. Baranowski, IEEE Trans. ED-13, 210 (1966).

[35] I. C. Irvin, IEEE Trans. ED-13, 208 (1966).

[36] L. S. Napoly, R. I. Ikova, Proc. IEEE 53, 1397 (1965). (1965).

[37] Electronics 4, 25, 1966.

[38] W. J. Matthei, Microwave J. 9, No. 3, 34 (1966).

[39] J. B. Gunn, International Science and Technology, No. 46, 43 (October, 1965).

[40] H. N. Toussaint, M. Krems, Proc. IEEE 53, 2113 (1965).

[41] B. Hoeffinger, IEEE Trans. ED-13, 151 (1966).

[42] A. L. Zakharov, Trudy soveshchaniya po udarnoĭ ionizatsii i tunel'nomu effektu v poluprovodnikakh (Proc. Conf. on Impact Ionization and Tunnel Effect in Semiconductors), Baku, IF AN USSR, 1962.

Translated by J. G. Adashko